Effects of pH and light exposure on the survival of bacteria and their ability to biodegrade organic compounds in clouds: Implications for microbial activity in acidic cloud water

Yushuo Liu,[1,2] Chee Kent Lim,[1] Zhiyong Shen,[1] Patrick K. H. Lee,[1,3] Theodora Nah[1,2,3*]

[1]*School of Energy and Environment, City University of Hong Kong, Hong Kong SAR, China*
[2]*Shenzhen Research Institute, Nanshan District, Shenzhen, China*
[3]*State Key Laboratory of Marine Pollution, City University of Hong Kong, Hong Kong SAR, China*

** To whom correspondence should be addressed: Theodora Nah (Email: theodora.nah@cityu.edu.hk)*

Abstract

Recent studies have reported that interactions between live bacteria and organic matter can potentially affect the carbon budget in clouds, which has important atmospheric and climate implications. However, bacteria in clouds are subject to a variety of atmospheric stressors, which can adversely affect their survival and energetic metabolism, and consequently their ability to biodegrade organic compounds. At present, the effects of cloud water pH and solar radiation on bacteria are not well understood. In this study, we investigated how cloud water pH (pH 3 to 6) and exposure to solar radiation impact the survival and energetic metabolism of two *Enterobacter* bacterial strains that were isolated from ambient air collected in Hong Kong and their ability to biodegrade organic acids. Experiments were conducted using simulated sunlight (wavelength 320 to 700 nm) and microcosms comprised of artificial cloud water that mimicked the pH and chemical composition of cloud water in Hong Kong, South China. Our results showed that the energetic metabolism and survival of both strains depended on the pH. Low survival rates were observed for both strains at pH < 4 regardless whether the strains were exposed to simulated sunlight. At pH 4 to 5, the energetic metabolism and survival of both strains were negatively impacted only when they were exposed to simulated sunlight. Organic compounds such as lipids and peptides were detected during exposure to simulated sunlight at pH 4 to 5. In contrast, there were minimal effects on the energetic metabolism and survival of both strains when they were exposed to simulated sunlight at pH > 5. The biodegradation of organic acids was found to depend on the presence (or absence) of simulated sunlight and the pH of the artificial cloud water medium. Overall, this study provides new insights into how two common atmospheric stressors, cloud water pH and exposure to solar radiation, can influence the survival and energetic metabolism of bacteria, and consequently the roles that they play in cloud processes.

Deleted: an aerosol sample

Deleted: carboxylic

Deleted: carboxylic

Deleted: Comparisons of the measured biodegradation rates to chemical reaction rates indicated that the concentrations of radical oxidants will also play important roles in dictating whether biodegradation processes can serve as a competitive sink for carboxylicorganic acids in cloud water. …

1. Introduction

Clouds are an important medium for the aqueous-phase formation and transformation of organic and inorganic compounds. In addition to inorganic and organic compounds, clouds contain biological matter including biological debris (e.g., dead cells, cell fragments) and live microorganisms (e.g., bacteria, fungal spores) (Bauer et al., 2002; Jaenicke, 2005; Burrows et al., 2009). Live microorganisms are mainly emitted directly into the atmosphere from natural sources (Jaenicke, 2005; Möhler et al., 2007; Burrows et al., 2009; Attard et al., 2012; Hu et al., 2018). Once airborne, they can participate in a variety of atmospheric processes such as cloud formation, precipitation, ice nucleation, and the microbial degradation of atmospheric organics (Amato et al., 2005; Delort et al., 2010; Vaitilingom et al., 2010; Vaitilingom et al., 2013; Morris et al., 2014; Morris et al., 2017; Hu et al., 2018; Huang et al., 2021; Zhang et al., 2021). Bacteria are incorporated into clouds through nucleation and scavenging processes (Möhler et al., 2007). So far, only bacterial communities in clouds in some areas (e.g., Puy de Dôme in France, Mt. Tai in North China) have been extensively investigated. These studies showed that the bacterial communities in clouds are highly complex and diverse, and mainly originate from vegetation, soil, and water bodies (Vaïtilingom et al., 2012; Wei et al., 2017; Zhu et al., 2018). A significant fraction of the bacteria in clouds may be major allergens and/or pathogens that originate mainly from anthropogenic activities, and their concentrations usually increase during air pollution episodes (Wei et al., 2017; Peng et al., 2019). The cell concentrations of bacteria in clouds typically range from about 10^2 to 10^5 cells mL^{-1} (Amato et al., 2005; Burrows et al., 2009; Amato et al., 2017). At present, our knowledge on bacterial communities in clouds are limited to the few areas that have been studied (e.g., Puy de Dôme in France, Mt. Tai in North China), (Amato et al., 2005; Amato et al., 2017; Wei et al., 2017; Péguilhan et al., 2021). Cultural bacteria typically makes up a very small fraction (about 1%) of the entire bacteria community in clouds (Amato et al., 2005).

Airborne bacteria are comprised of both dead or dormant cells and metabolically active cells. Previous culture-based and culture-independent analyses of bacteria isolated from cloud water have shown that some of these bacteria species are metabolically active (Amato et al., 2007; Krumins et al., 2014; Amato et al., 2019). Previous studies have reported that the

Deleted: and microbiological-ecosystem interactions

Deleted: However, a

Deleted: metabolically active

Deleted: ,

Deleted: and only to cultural bacteria which typically makes up about 1% of the entire bacteria community

degradation of organic compounds as a result of microbiological-chemical interactions between live bacteria and organic matter can play an important role in influencing the carbon budget in clouds, which will have important atmospheric and climate implications (Delort et al., 2010; Vaitilingom et al., 2010; Vaitilingom et al., 2013; Ervens and Amato, 2020). Many bacteria species have the enzymes needed to biodegrade organic compounds. Some of the bacteria species isolated from cloud water could biodegrade organic acids, formaldehyde, methanol, phenolic compounds, and amino acids (Ariya et al., 2002; Husárová et al., 2011; Vaïtilingom et al., 2011; Jaber et al., 2020; Jaber et al., 2021). However, the bacteria are exposed to a variety of stressors that can negatively impact their survival and microbial activity in clouds. Joly et al. (2015) previously investigated the individual impacts of osmotic shocks, freeze-thaw cycles, and exposure to light and H_2O_2 on the survival of different bacterial strains in microcosms mimicking cloud water chemical composition at Puy de Dôme. Osmotic shocks and freeze-thaw cycles reportedly had the greatest negative impacts on the survival of bacteria, while exposure to light and H_2O_2 had limited impacts on the survival of bacteria. However, there are other stressors that bacteria in clouds are commonly subjected to beyond the four stressors investigated by Joly et al. (2015). In addition, when combined together, the stressors may have synergistic negative impacts on the survival and microbial activity of bacteria in clouds. The potentially synergistic negative impacts that stressors have on the survival and microbial activity of bacteria in clouds have yet to be investigated. Some bacteria species respond to stressors by releasing organic compounds (e.g., proteins, pigments, lipids) as a defensive mechanism (Davey and O'toole, 2000; Delort et al., 2010; Flemming and Wingender, 2010; Vaïtilingom et al., 2012; Matulova et al., 2014). When bacteria species cannot withstand the stress, the resulting cellular damage and lysis will lead to the release of biological material. In addition, the ability of bacteria to biodegrade organic compounds in clouds will decrease if their metabolism and survival are negatively impacted.

Cloud water acidity is another stressor that bacteria are subjected to in clouds. There has been limited study on the impact of cloud water pH on the survival and microbial activity of bacteria in clouds. However, some studies have reported that the cloud water pH impacts the diversity and composition of bacterial communities (Amato et al., 2005; Peng et al., 2019).

Deleted: isolated from cloud water

Deleted: such as carboxylic

Deleted:

Deleted: In addition to having the appropriate enzymes, the bacteria need to be metabolically active to biodegrade organic compounds.

Deleted: the

Deleted: influences

For instance, spore-forming bacteria were abundant in pH 4.9 cloud water at Puy de Dôme, while more diverse and higher concentrations of non-spore-forming bacteria were observed in pH 5.8 cloud water (Amato et al., 2005). The pH of cloud water typically lies between 3 and 6 (Pye et al., 2020), with a global mean of around pH 5.2 (Shah et al., 2020). Areas with high inputs of sulfuric acid and/or nitric acid combined with low inputs of ammonia, dust, and sea salt, especially in parts of East Asia, have moderately acidic to highly acidic cloud water (pH < 5) (Li et al., 2020; Pye et al., 2020; Shah et al., 2020; Qu and Han, 2021). To the best of our knowledge, there has been no studies on how moderately acidic to highly acidic cloud water affects the survival and microbial activity of bacteria. The effects of light exposure on the survival and microbial activity of bacteria are also ambiguous. Some studies reported that exposure to UVA and visible light will lead to the formation of intracellular reactive oxidative species, which can damage important cell components and cause cell death (Anglada et al., 2015). However, exposure to light reportedly did not impact the survival rates of bacterial strains from *Pseudomonas syringae*, *Arthrobacter* sp., and *Sphingomonas* sp. (Joly et al., 2015). While it is possible that exposure to acidic cloud water and light have a synergistic effect on the survival and microbial activity of bacteria, previous laboratory investigations were mainly performed in microcosms with the pH set between 5 to 7 to mimic cloud water in areas that have high inputs of ammonia, dust, and sea salt, such as the Puy de Dôme (Vaïtilingom et al., 2011; Joly et al., 2015; Jaber et al., 2021; Jaber et al., 2020).

This study investigates how cloud water pH and exposure to solar radiation affect the survival and energetic metabolism of bacteria and their ability to biodegrade organic compounds in clouds. We designed a series of laboratory experiments in microcosms containing artificial cloud water that mimicked the pH and chemical composition of atmospheric cloud water collected at the Tai Mo Shan station in Hong Kong, South China. South China is a region with moderately acidic to highly acidic cloud water due to its higher concentrations of acidic ions (e.g., SO_4^{2-}, NO_3^-) compared to alkaline ions (e.g., NH_4^+, Ca^{2+}) (Li et al., 2020; Qu and Han, 2021). Different pH (pH 3.3 to 5.9) and irradiation (illuminated vs. dark) conditions were employed in the experiments, during which we analyzed the biological material and organic compounds in the artificial cloud water medium at different

reaction time points. Since cloud water bacterial isolates from the Tai Mo Shan station are not available, two *Enterobacter* bacterial strains that were isolated from ambient air in Hong Kong were used as model bacteria in this study. In general, our current knowledge of the diversity and composition of bacteria communities in cloud water in Hong Kong and South China is very limited due to the scarcity of characterization studies conducted in this region. Results from a previous study reported that *Enterobacter* was one of the bacteria species in cloud water collected at the Nanling Mountain station in South China (Peng et al., 2019). *Enterobacter* bacteria has been detected in urban aerosols in different parts of the world, including South China (Chen et al., 2012; Després et al., 2012; Ding et al., 2015; Zhou et al., 2018; Prokof'eva et al., 2021). In addition, the enrichment of *Enterobacter* bacteria in the atmosphere during air pollution episodes has been reported in parts of Asia, America, and Europe (Romano et al., 2019; Ruiz-Gil et al., 2020; Romano et al., 2021). Since organic acids are ubiquitous in clouds (Tsai and Kuo, 2013; Löflund et al., 2002; Sun et al., 2016; Li et al., 2020) and can be biodegraded by most bacteria (Vaitilingom et al., 2010; Vaïtilingom et al., 2011), we chose seven organic acids that are commonly detected in clouds (formic acid, acetic acid, oxalic acid, maleic acid, malonic acid, glutaric acid, and methanesulfonic acid) as model organic compounds for our investigations of how cloud water pH and light exposure affect the ability of bacteria to biodegrade organic compounds in clouds.

Deleted: an aerosol sample

Deleted: suggested

Deleted: *Enterobacter* bacteria is pathogenic, and they originate mainly from anthropogenic activities.

Deleted: carboxylic

Deleted: carboxylic

Deleted: maleaic

2. Methods

2.1. Strain isolation and whole genome sequencing

Two new strains (B0910 and pf0910) belonging to *Enterobacter* species were isolated by exposing nutrient agar plates to ambient air in an urban environment (22.3360° N, 114.1732° E) at a height of 50 m above sea level during the summer season (~22 ℃) in Hong Kong. The genomes of the two strains were sequenced using a GridION sequencer (Oxford Nanopore Technologies) by following the manufacturer's workflow. Genome assembly and the downstream genomic analyses are described in detail in Section S1. Based on genome comparison, *E. hormaechei* B0910 is most similar to *Enterobacter hormaechei* subsp. *hoffmannii* DSM 14563 (Average Nucleotide Identity (ANI) = 98.92) and *E. hormaechei*

Deleted: .

Deleted: the

Deleted: eter

Deleted: from the

Deleted: ,

Deleted: in

Deleted: from an aerosol sample collected in Hong Kong using repeated plating on Luria broth (LB) agar.

pf0910 to *Enterobacter hormaechei* subsp. *steigerwaltii* DSM 16691 (ANI = 98.73) (Figure S1). *E. hormaechei* B0910 has a chromosome (4.69 Mbp) with 4875 coding sequences (CDSs) and a single plasmid (373 Kbp) with 383 CDSs. *E. hormaechei* pf0910 strain has a chromosome (4.78 Mbp) with 5072 CDSs and two plasmids of 281 Kbp (344 CDSs) and 73 Kbp (79 CDSs).

2.2. General experimental approach

To simulate cloud water conditions in Hong Kong, artificial cloud water containing major organic and inorganic ions in cloud water previously collected at the Tai Mo Shan station (TMS; 22°24'N, 114°16'E, 957 m a.s.l.) were used in each experiment. Organic (acetic acid, formic acid, oxalic acid, pyruvic acid) and inorganic (magnesium chloride, calcium chloride, potassium chloride, sodium chloride, ammonium sulfate, ammonium nitrate, sodium hydroxide and hydrochloric acid) compounds were used to prepare the artificial cloud water. Experiments were performed using a Rayonet photoreactor (RPR-200, Southern New England Ultraviolet Company). We followed the method employed in previous studies (George et al., 2015; Huang et al., 2018; Misovich et al., 2021; Li et al., 2022) and used eight lamps with outputs centered at different wavelengths to roughly simulate the range of solar radiation wavelengths (320 to 700 nm) inside the photoreactor. Figure S2 shows the resulting photon flux inside the photoreactor. The temperature (25 ℃) during the experiment was regulated by a fan located at the bottom of the photoreactor.

The two strains were grown in LB broth at 37 ℃ to stationary phase. The culture was then centrifuged at 6000 rpm for 10 min at 4 ℃ and the cell pellets were rinsed with artificial cloud water (Table S1) three times. For investigations of the time evolution in the survival and energetic metabolism of bacteria at different pH under illuminated vs. dark conditions (Section 2.2), the cells were re-suspended in artificial cloud water to an initial concentration of ~10^5 cells mL^{-1}. For investigations of the biodegradation of organic acids by bacteria at different pH under illuminated vs. dark conditions (Section 2.3), the cells were re-suspended in artificial cloud water to an initial concentration of ~10^6 cells mL^{-1}. A calibration curve was used to convert between optical density and bacterial cell concentration.

Deleted: carboxylic

Quartz tubes containing bacterial cells suspended in artificial cloud water (5 mL) were placed on a rotating vial rack in the middle of the photoreactor. The quartz tubes for the dark control experiments were wrapped in aluminum foil and placed inside the photoreactor. The pH of the artificial cloud water did not change significantly during the experiments. Aliquots of the solutions were taken at every hour over 12 hours for various offline chemical analyses. Colony Forming Unit (CFU) counts on LB agar at 37 °C for 16 hours was also performed to determine the culturable bacterial cell concentrations, which was used to calculate the bacteria survival rates. The adenosine diphosphate/adenosine triphosphate (ADP/ATP) ratios were measured using an assay kit (EnzyLight™, BioAssay Systems) and a biolumineter (SpectraMax M2e) to determine changes in the bacteria energetic metabolism. All the experiments and measurements were performed in triplicates

Deleted: A

Deleted: D

Deleted: A

Deleted: T

2.3. Investigations of the survival and energetic metabolism of bacteria at different pH under illuminated vs. dark conditions

Six pH conditions (pH 3.3, 4.3, 4.5, 4.7, 5.2 and 5.9) were chosen for this set of experiments, which were performed under both dark and illuminated conditions. The six pH conditions investigated fall within the range of pH values for cloud water previously measured at Tai Mo Shan (pH 3.0 to 5.9) (Li et al., 2020). The pH of the artificial cloud water used to suspend the bacterial cells was adjusted using sodium hydroxide and hydrochloric acid. Table S1 shows the resulting concentrations of organic and inorganic ions in the artificial cloud water used in these experiments, which are similar to those in cloud water collected at Tai Mo Shan by Li et al. (2020).

During some experiments, aliquots of the solutions were taken at time points 0 h, 2 h, 4 h, 8 h, and 12 h and analyzed by ultra-performance liquid chromatography-mass spectrometry (UPLC-MS). Each aliquot of solution was first passed through a 0.22 µm filter to remove intact bacterial cells. Water-insoluble and water-soluble biological material and organic compounds were then extracted from these filtered solutions using the method described in Section S2. 200 µL of the extract was then transferred into glass vial inserts for UPLC-MS analysis. Non-targeted UPLC-MS analysis was performed using an ultrahigh performance liquid

chromatography system (ExionLC AD system, Sciex) coupled to a high-resolution quadrupole-time-of-flight mass spectrometer (TripleTOF 6600 system, Sciex) equipped with electrospray ionization (ESI). Chromatographic separation was performed on a Kinetex HILIC LC column (100 × 2.1 mm, 2.6 µm, 100 Å, Phenomenex) using positive ESI mode. Since very low signals were obtained for negative ESI mode, we did not use it for our analysis. Details about the UPLC-MS operation, data processing, and statistical analysis can be found in Section S3.

2.4. Investigations of the biodegradation of organic acids at different pH under illuminated vs. dark conditions

The biodegradation of seven organic acids (formic acid, acetic acid, oxalic acid, maleaic acid, malonic acid, glutaric acid, and methanesulfonic acid (MSA)) that were mixed together were measured at pH 4.3 and pH 5.9 under both dark and illuminated conditions. The concentrations for each of the forementioned organic acids in cloud water and rain water typically fall within the range of 1 to 10 µM (Tsai and Kuo, 2013; Löflund et al., 2002; Sun et al., 2016; Li et al., 2020). Due to the detection limits of the IC system used to measure the organic acids, the concentration for each organic acid was set to 50 µM (Table S2), which is around 10 times higher than the concentrations typically measured in cloud water. The concentrations of inorganic ions in the artificial cloud water were also increased by 10 times. Vaitilingom et al. (2010) previously reported that the same biodegradation rates will be obtained as long as the concentration ratio of the chemical compounds to bacterial cells is constant. However, the authors drew this conclusion based on experiments performed using a *Pseudomonas graminis* bacterial strain incubated in the presence of a single organic compound as the carbon source. At present, it is unclear whether this conclusion can be extrapolated to other bacteria species incubated in the presence of multiple organic compounds, and this warrants further study. Nevertheless, we made the same assumption (i.e., the same biodegradation rates will be obtained as long as the concentration ratio of the chemical compounds to bacterial cells is constant) as was done in previous studies that investigated the biodegradation of multiple organic compounds by different bacteria species (Vaïtilingom et al., 2011; Jaber et al., 2020; Jaber et al., 2021). Hence, the bacteria concentration used was set to 10^6 cells mL^{-1} to maintain the same concentration ratio of the organic acids to bacterial cells.

Deleted: carboxylic

Deleted: carboxylic

Deleted: carboxylic

Deleted: carboxylic

Deleted: carboxylic

Deleted: Previous studies have

Deleted: carboxylic

Table S2 shows the resulting concentrations of the organic and inorganic ions in the artificial cloud water used in these experiments.

During each experiment, aliquots of the solutions were taken every 2 hours over 12 hours. The organic acid concentrations in each filtered aliquot of solution were measured by ion chromatography (IC) using a Dionex ICS-1100 (ThermoFisher Scientific) system. Details of the IC operation can be found in Section S4. To calculate the initial biodegradation rate, the time evolution of each organic acid concentration over 12 h was plotted and fitted with the following equation (Vaïtilingom et al., 2011; Jaber et al., 2020; Jaber et al., 2021):

$$\ln\left(\frac{C}{C_0}\right) = f(t) = -k \times t \quad (1)$$

where k (s^{-1}) is the rate constant obtained from the exponential fit to the decay of the organic acid. The following equation was used to calculate the biodegradation rate per bacteria cell (R):

$$\mathrm{R} = \frac{k \times C_0}{[Cell]_{experiment}}, (mol\ cell^{-1} s^{-1}) \quad (2)$$

where C_0 $(mol \cdot L^{-1})$ is the initial concentration of the organic acid, $[Cell]_{experiment}$ $(cell \cdot L^{-1})$ is the concentration of bacterial cells in the experiment. Control experiments were performed under illuminated and dark conditions using solutions that contained organic acids but no bacterial cells. The organic acids did not degrade in these control experiments.

3. Results and discussion

3.1. Impact of pH on the survival and energetic metabolism of bacteria under illuminated and dark conditions

Figure 1 shows the survival rates and ADP/ATP ratios of the *E. hormaechei* B0910 and *E. hormaechei* pf0910 strains over time under illuminated and dark conditions at different artificial cloud water pH. The ADP/ATP ratio is used as an indicator of the bacteria's metabolic activity and survival rate in this study. Growing cells usually maintain a constant ADP/ATP ratio because whenever there is a decrease in intracellular ATP production, its degradation product ADP will be resynthesized to form ATP to maintain intracellular ATP concentrations (Koutny et al., 2006; Guan and Liu, 2020). In contrast, when there is a disruption in the metabolism of ATP production, ATP cannot be resynthesized from ADP even though ATP is

Deleted: carboxylic

Deleted: carboxylic

Deleted: carboxylic

Deleted: carboxylic

Deleted: light

Deleted: carboxylic

Deleted: carboxylic

Deleted: with normal functioning cells usually maintaining a constant ADP/ATP ratio

Deleted: This is because

Deleted: However

still converted to ADP, which will cause the ADP/ATP ratio to increase (Koutny et al., 2006; Guan and Liu, 2020).

The artificial cloud water pH clearly had a significant effect on the survival rates and ADP/ATP ratios of the two strains. At pH 3.3, the concentrations of viable cells decreased to zero after 20 minutes regardless whether the strains were exposed to light. For pH 4.3, 4.5 and 4.7, the survival and ADP/ATP ratios of the two strains depended on whether they were exposed to light. There were no significant changes in the survival rates and ADP/ATP ratios for both strains under dark conditions. In contrast, the concentrations of viable cells for both strains gradually decreased when they were exposed to light. Consistent with the lower survival rates, the ADP/ATP ratios for both strains increased over time. The survival rates and ADP/ATP ratios were the lowest and highest, respectively, at pH 4.3 after 12 h of illumination. There were no significant changes in the survival rates and ADP/ATP ratios of both strains at pH 5.2 and 5.9 under illuminated and dark conditions.

Deleted: T

Deleted: also

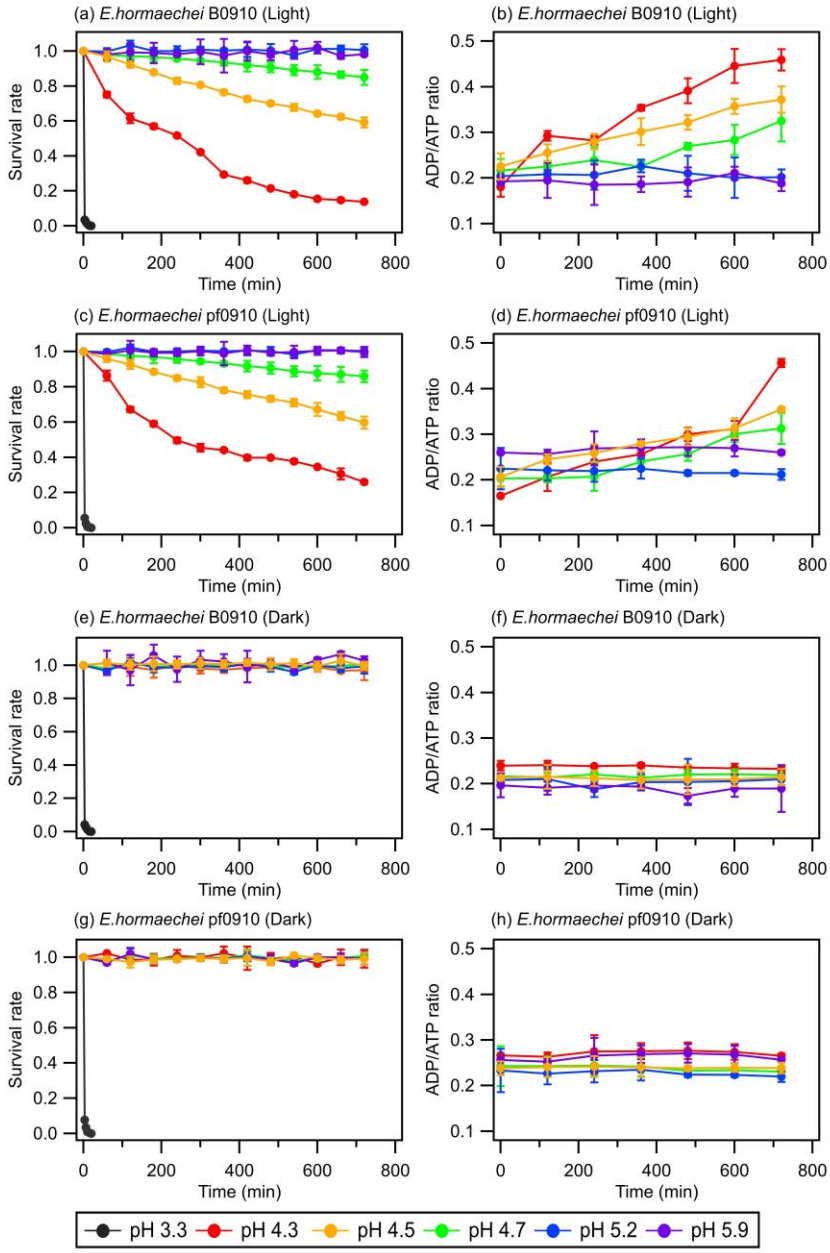

340

341 **Figure 1.** Survival rates and ADP/ATP ratios of the *E. hormaechei* B0910 and *E. hormaechei*

342 pf0910 strains at pH 3.3 to pH 5.9 under illuminated and dark conditions over time. The

survival rate is defined as the number concentration of culturable viable cells divided by the initial number concentration of culturable viable cells at time point 0 min. Error bars represent one standard deviation from the mean of biological triplicates.

Figure 1 clearly shows that the artificial cloud water pH and exposure to light can have a synergistic effect on the survival and energetic metabolism of *E. hormaechei* B0910 and *E. hormaechei* pf0910. Based on these results, both strains will likely survive during the daytime and nighttime in pH > 5 cloud water. However, cloud water pH will play an important role in dictating the fraction of the bacteria that will survive in the daytime at pH 4 to 5. A low pH environment can lower the internal pH of cells, which affects essential pH-dependent biological and cellular functions such as decreased enzymatic activity, compromised cellular processes (e.g., central metabolic pathways, ATP production), and protein denaturation in cells (Bearson et al., 1997; Lund et al., 2014). Our genomic analysis revealed that the two strains have genes encoding a F1F0-type ATP synthase, which can export protons from their cytoplasm to cope with pH stress (Krulwich et al., 2011). In addition, genes encoding potassium transporters, which may be involved in pH homeostasis (i.e., both Kup-type low-affinity and Kdp-type high-affinity potassium transporters) (Brzoska et al., 2022) were found in the genome of both strains (Table S3). Our results indicated that both strains will likely survive in pH 4 to 5 cloud water at night. However, being in cloud water at pH 4 to 5 will likely negatively impact the ability of cells to tolerate sunlight, which will affect their survival during the daytime. Based on our results, we estimate that the half-lives of the bacteria strains in pH 4.3 cloud water under illumination conditions (e.g., light intensity, wavelengths) similar to those in our study are around 430 min. The half-lives of the bacteria strains in pH < 4 are cloud water are lower. Based on our results, we estimate that the daytime and nighttime half-lives of the bacteria strains in pH 3.3 cloud water are around 2 min.

Deleted: , respectively

Deleted: (Brzoska et al., 2022)

3.2. Compounds released by bacteria under acidic and illuminated conditions

Some bacteria species adapt to sunlight exposure and acidic environments by deploying adaptation strategies and defensive mechanisms such as undergoing DNA repair, aggregation-promoting, and pigmentation mechanisms (Bearson et al., 1997; Davey and O'toole, 2000;

Delort et al., 2010; Flemming and Wingender, 2010; Vaïtilingom et al., 2012; Matulova et al., 2014; Guan and Liu, 2020). Some of these adaptation strategies and defensive mechanisms will cause the bacteria to release organic compounds into cloud water (Davey and O'toole, 2000; Delort et al., 2010; Flemming and Wingender, 2010; Vaïtilingom et al., 2012; Matulova et al., 2014). In addition, bacterial cellular damage and lysis will lead to the release of biological material and organic compounds. To investigate the compounds released by *E. hormaechei* B0910 and *E. hormaechei* pf0910 during exposure to light and acidic environments, we used UPLC-MS to analyze the solutions in experiments where pH 4.3 and pH 5.9 artificial cloud water were used. The UPLC-MS measurements revealed that cell lysis led to the release of water-soluble and water-insoluble compounds when the two strains were exposed to light at pH 4.3. The quantities of these compounds changed with light exposure time. In contrast, no water-soluble and water-insoluble compounds were detected in the solutions of the two strains under dark conditions at pH 4.3, and under dark and illuminated conditions at pH 5.9. This suggested that these two strains did not release organic compounds and the cells remained intact under these conditions. It is also possible that these two strains released organic compounds as an adaption strategy and/or defensive mechanism but the concentrations of these compounds were below the detection limits of our UPLC-MS instrument.

Deleted: production

Principal component analysis (PCA) with 95% confidence ellipse was applied to the UPLC-MS data of the detected water-soluble and water-insoluble compounds to identify discriminations between samples with different light exposure times. In each PCA plot (Figure 2), samples with the same light exposure time clustered together. While there was slight overlap between some of the clusters in the PCA plots, the clusters were mostly separated from one another. Partial least squares discrimination analysis (PLS-DA) was applied to the UPLC-MS data to identify water-soluble and water-insoluble compounds that showed significant changes in their relative abundances during exposure to light. 259 water-soluble compounds and 215 water-insoluble compounds were identified for *E. hormaechei* B0910 (Figure S3), while 209 water-soluble compounds and 251 water-insoluble compounds were identified for *E. hormaechei* pf0910 (Figure S4). We identified the molecular formulas and chemical structures of 78 water-soluble compounds and 144 water-insoluble compounds released by *E. hormaechei*

B0910, and 118 water-soluble compounds and 114 water-insoluble compounds released by *E. hormaechei* pf0910. These identified compounds were subsequently classified into different classes based on their chemical functionalities.

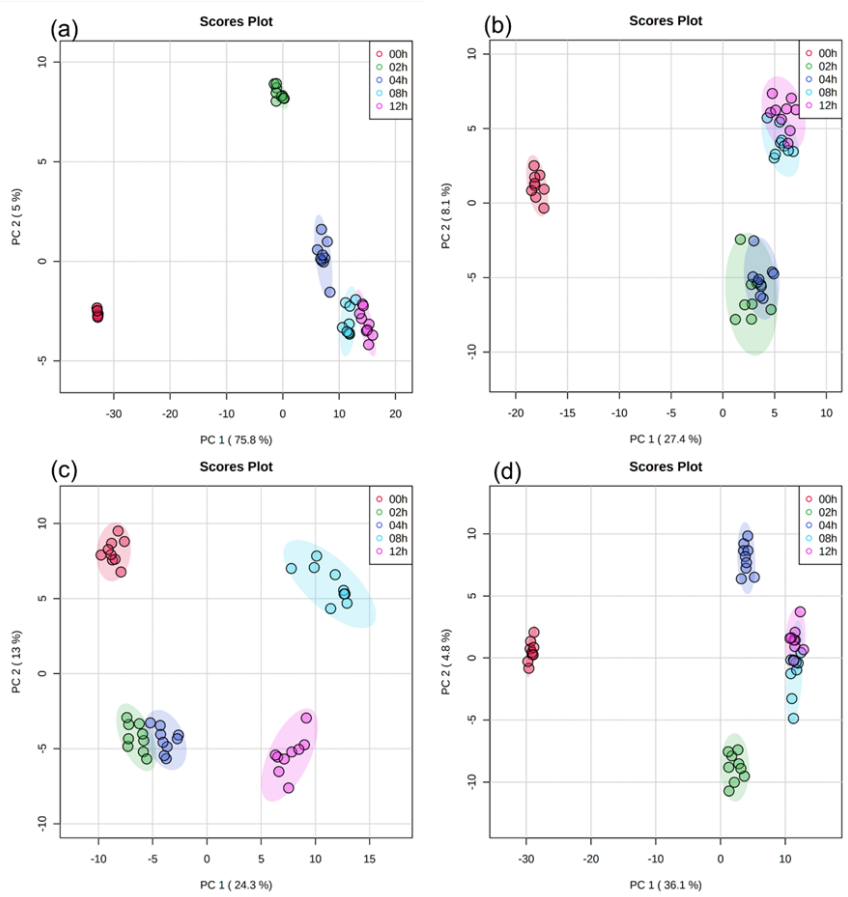

Figure 2. PCA results of UPLC-MS data: (a) water-soluble compounds and (b) water-insoluble compounds from *E. hormaechei* B0910, and (c) water-soluble compounds and (d) water-insoluble compounds from *E. hormaechei* pf0910 during exposure to light at pH 4.3. Each cluster representing a different light exposure time (i.e., 0 h, 2 h, 4 h, 8 h, and 12 h) has nine points since three samples were taken at each light exposure time, and UPLC-MS analysis was performed in triplicate for each sample.

Figures 3 and S5 show the time evolution of the UPLC-MS total ion chromatograph (TIC) signals of the different classes of water-soluble and water-insoluble compounds released by *E. hormaechei* B0910 and *E. hormaechei* pf0910 over time, respectively. The UPLC-MS TIC signals of the classes of water-soluble and water-insoluble compounds released by the two strains increased with light exposure time. The increase in the UPLC-MS TIC signals coincided with the decrease in the bacteria survival rate and the increase in the ADP/ATP ratio. Even though the heatmaps showed that some of the compounds had noticeable changes in their relative abundances during exposure to light (Figures S3 and S4), the relative abundances of the different classes of compounds contributed to the total TIC at each time point did not change substantially (Figures S6 and S7).

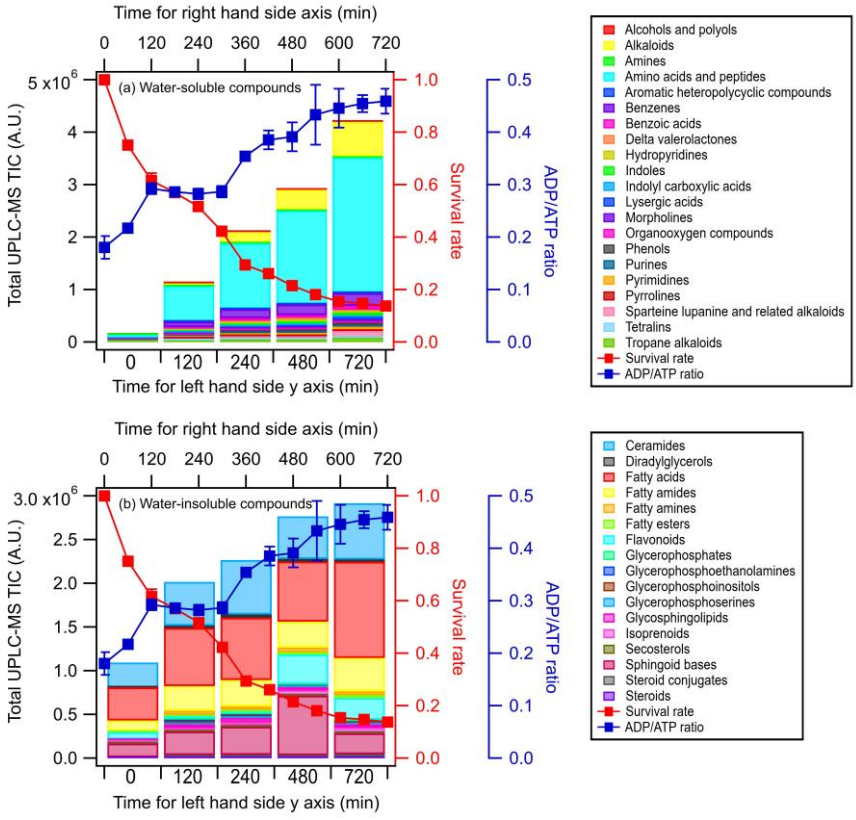

Figure 3. Time evolution of the UPLC-MS total ion chromatograph (TIC) signals of (a) water-soluble compounds, and (b) water-insoluble compounds from *E. hormaechei* B0910 during exposure to light at pH 4.3 over time. These compounds are classified based on their chemical functionality. Also shown are the time evolution of the survival rate and ADP/ATP ratio of *E. hormaechei* B0910.

To better understand the compounds released by the two strains, the O/C and H/C elemental ratios of the identified compounds were used to construct Van Krevelen (VK) diagrams. Regions of the VK diagrams were assigned to eight chemical classes based on the combined O/C and H/C ratios: lipids, unsaturated hydrocarbons, condensed aromatic structures, peptides, lignin, tannin, amino sugars, and carbohydrates (Table S4) (Bianco et al., 2018; Laszakovits and Mackay, 2022). Rivas-Ubach et al. (2018) previously reported that the region of the VK diagram assigned to amino sugars overlaps with the region for nucleic acids. Figures S8 and S9 show the VK diagrams for water-soluble and water-insoluble compounds released by *E. hormaechei* B0910, respectively, while Figures S10 and S11 show the VK diagrams for water-soluble and water-insoluble compounds released by *E. hormaechei* pf0910, respectively. Majority of the water-soluble and water-insoluble compounds released from both strains (50% to 60%) were assigned as lipids based on their O/C and H/C ratios, while the second most abundant compound class was peptides (10% to 20%). The two least abundant compound classes were amino sugars/nucleic acids and carbohydrates. Since the dry matter of a typical bacterial cell contains approximately 55% proteins and amino acids, 24% nucleic acids, 10% carbohydrates, 7% lipids, and 5% inorganic minerals and trace elements (Watson et al., 2007), the differences in the abundance of compound classes detected vs. the dry matter of a typical bacterial cell indicated that cellular components were likely biologically and/or chemically modified during and after cell lysis during exposure to light. For instance, the large abundance of peptides detected could be a result of biological and/or chemical modifications of proteins and amino acids, which comprise majority of the dry matter of a typical bacterial cell. Peptide bonds are formed by biochemical reactions where a water molecule is removed as the amino group of one amino acid is joined to the carboxyl group of a neighboring amino acid. The large abundance of lipids was unsurprising since lipids are the main component of cell

Deleted: S3

Deleted: .

Deleted: This was unsurprising since lipids are the main component of cell membranes so large quantities of lipids are expected from the lysed cells.

Deleted: T

Deleted: , which were likely formed from biological and/or chemical modifications of proteins

membranes so large quantities of lipids are expected from the lysed cells. Most of the lipid molecules released during cell lysis may not have undergone biological and/or chemical modifications under our experimental conditions. The two least abundant compound classes were amino sugars/nucleic acids and carbohydrates. This was somewhat surprising since nucleic acids and carbohydrates are abundant in the dry matter of a typical bacterial cell. It is possible that these compounds were biologically and/or chemically modified to form other compounds (e.g., exopolymeric substances) during exposure to light (Matulova et al., 2014). In addition, the extraction procedure employed (Section S2) may not have extracted these compounds effectively for analysis. For instance, nucleic acids and carbohydrates are polar molecules, which are difficult to retain on the solid phase extraction columns used in this study. These compounds may also have been poorly separated in UPLC and/or inefficiently ionized by ESI.

These detected compounds indicated that bacterial cell lysis could be a source for carbon in cloud water. Many of the compound classes detected in this study have previously been measured in atmospheric cloud water. For instance, large abundances of peptide-like compounds and lipid-like compounds have been measured in cloud water from Puy de Dôme (Bianco et al., 2018; Bianco et al., 2019), which is consistent with the detection of large abundances of compounds assigned to the peptide and lipid compound classes in this study. This suggested that peptide-like and lipid-like compounds could be used as biomarkers to evaluate bacterial contributions to atmospheric samples. Previous studies have used fatty acids, which are integral building blocks of lipids, in atmospheric samples as biomarkers for characterizing and quantifying bacteria, and assessing the atmospheric transport of bacteria (Kawamura et al., 2003; Lee et al., 2004; Tyagi et al., 2015). While this study shows that bacterial cell lysis will release large quantities of peptide-like and lipid-like compounds, using these compounds as biomarkers for bacterial cell lysis in atmospheric samples will likely be complex as the concentrations of these compounds will likely change with time. This is because peptide-like and lipid-like compounds will undergo chemical and biological transformations after they have been released during cell lysis, which will impact their concentrations in atmospheric samples. Amino acids, which are building blocks of peptides, are known to

Deleted: The

Deleted: amino sugars

Deleted: form

Deleted: important

Deleted: constituents

Deleted: of cells

undergo chemical reactions with oxidants in cloud water, (Bianco et al., 2016). In addition, peptide-like and lipid-like compounds can be produced and/or consumed by cloud microorganisms to maintain their metabolism (Bianco et al., 2019; Jaber et al., 2021).

3.3. Impact of pH on the biodegradation of organic acids by bacteria under illuminated and dark conditions

The biodegradation of seven organic acids (i.e., formic acid, acetic acid, oxalic acid, maleic acid, malonic acid, glutaric acid and MSA) that were mixed together were measured under dark and illuminated conditions at pH 4.3 and pH 5.9. Only some of the seven organic acids were biodegraded by the two strains. Based on our experimental conditions (liquid water content $\approx 10^{12}$ µg m^{-3}, the density of water) and the organic acids' Henry's law constants, these organic acids will be in the aqueous phase and are not expected to volatilize during these experiments. Thus, the observed decays were due to bacterial metabolism. *E. hormaechei* B0910 biodegraded formate and oxalate under dark and illuminated conditions at pH 4.3 and pH 5.9, and biodegraded malonate and maleate only under dark conditions at pH 4.3 and pH 5.9. In contrast, *E. hormaechei* pf0910 biodegraded only formate and oxalate under dark and illuminated conditions at pH 4.3 and pH 5.9. Biodegradation was not observed for acetate, MSA, and glutarate.

Table S5 summarizes the enzymes or metabolic pathways related to the biodegradation of organic acids in the two strains. Genes encoding formate dehydrogenases were identified in both genomes, which is consistent with the observed formate biodegradation. However, no known genes for oxalic acid biodegradation (Liu et al., 2021) were found in the genomes of both strains, which suggested the presence of yet to be characterized pathways that catalyzed the biodegradation. Interestingly, a protein with Cupin 2 domain was found in both genomes. The Cupin superfamily consists of a diverse range of enzymes including oxalate oxidase and oxalate decarboxylase that can biodegrade oxalic acid (Burrell et al., 2007).

Only the *E. hormaechei* B0910 strain was observed to biodegrade malonic acid. Interestingly, the malonyl-CoA-acyl carrier transcacylase observed in the *E. hormaechei* pf0910 strain seems to be a fusion protein, which may render it ineffective in utilizing malonic

Deleted: carboxylic

Deleted: carboxylic

Deleted: carboxylic

Deleted: Section S5 and Table S4 discuss the enzymes and metabolic mechanisms associated with the biodegradation of carboxylic acids by the two strains.

Deleted: 4

Deleted: d

Deleted: carboxylic

acid. Although no gene encoding maleate isomerase was identified in the genomes of both strains, the maleic acid biodegradation observed can be attributed to the activity of other enzymes with broad substrates specificity (Hatakeyama et al., 2000). The genes encoding for the small and large protein subunits that together form the 3-isopropylmalate dehydratase, the enzyme that isomerizes 2-isopropylmalate to 3-isopropylmalate, were found in both the *Enterobacter* strains. The small and large protein subunits of this enzyme are homologous to the small (51% amino acid identity) and large (59% amino acid identity) protein subunit constituents of maleate hydratase (HbzIJ) from *Pseudomonas alcaligenes* NCIMB 9867 that converts maleate to D-malate (Liu et al., 2015). Given the high protein homology, we speculate that the 3-isopropylmalate dehydratase in the *Enterobacter* strains may have a broader substrate specificity than known and it may be able to biodegrade maleate.

The lack of biodegradation of acetic acid, MSA, and glutaric acid in the experiments could be partly explained by the genomic information. Both strains have genes that encode enzymes involved in the biodegradation (Table S5) and associated uptake transporters (i.e., acetate permease (ActP) and succinate-acetate/proton symporter (SatP)) of acetic acid. The lack of the corresponding biodegradation in the experiments could be due to the low uptake of acetic acid by cells as ActP functions to scavenge low concentrations of the compound (Gimenez et al., 2003) while SatP could be inhibited by formic acid found in the cloud water medium (Sá-Pessoa et al., 2013). Genes encoding the two-component alkanesulfonate monooxygenase for MSA biodegradation were found in both strains, but they were likely not expressed as sulfur was not deficient in the cloud water medium (Kahnert et al., 2000; Eichhorn and Leisinger, 2001), which is consistent with the absence of MSA biodegradation in the experiments. While genes encoding succinate-semialdehyde dehydrogenase/glutarate-semialdehyde dehydrogenase, which display a reversible conversion between glutarate-semialdehyde and glutarate in the KEGG database (Kanehisa et al., 2022), were found in both strains, to the best of our knowledge there is no report of experimental results confirming that the reaction can go in the reverse direction from glutarate to glutarate-semialdehyde. In addition, a study of glutaric semialdehyde dehydrogenase reported the irreversible nature of

Deleted: 4

the catalysis of glutarate semialdehyde to glutarate (Ichihara and Ichihara, 1961). Thus, it is not surprising that glutarate biodegradation was not observed for the two strains.

Figure 4 summarizes the measured biodegradation rates of the organic acids for the two strains under dark and illuminated conditions at pH 4.3 and pH 5.9. These biodegradation rates were determined from fits to the decays of the organic acids from reaction time 0 to 12 hour in each experiment (Section 2.4). The measured biodegradation rates were around 10^{-19} to 10^{-18} mol cell^{-1} s^{-1}, which were on the same order of magnitude as the bacterial strains isolated from cloud water and implemented into cloud models (Vaitilingom et al., 2010; Vaïtilingom et al., 2011; Fankhauser et al., 2019). Although both strains were affiliated to *E. hormaechei*, the artificial cloud water pH and exposure to light impacted their biodegradation of organic acids differently. The rates at which formate and oxalate were biodegraded by *E. hormaechei* B0910 had the following order: dark conditions at pH 5.9 > illuminated conditions at pH 5.9 > dark conditions at pH 4.3 > illuminated conditions at pH 4.3. This order was different for *E. hormaechei* pf0910: dark conditions at pH 5.9 > dark conditions at pH 4.3 > illuminated conditions at pH 5.9 > illuminated conditions at pH 4.3. Despite the effects that the artificial cloud water pH and exposure to light had on the formate and oxalate biodegradation, the fastest and slowest biodegradation rates only differed by a factor of 1.4 to 3.7. Figure S12 compares the biodegradation rates measured at pH 4.3 vs. pH 5.9, and under illuminated vs. dark conditions. For the effect of artificial cloud water pH on the biodegradation of organic acids by *E. hormaechei* B0910, the differences in the biodegradation rates were statistically significant for the four acids (Student's t test, p value < 0.05). Conversely, the differences in the biodegradation rates of formate and oxalate as a result of light exposure were statistically significant at pH 5.9 (Student's t test, p value < 0.05). For the effect of artificial cloud water pH on the biodegradation of organic acids by *E. hormaechei* pf0910, only the difference in the dark biodegradation of oxalate was statistically significant (Student's t test, p value < 0.05). In contrast, light exposure reduced the formate biodegradation rates significantly at both pH 4.3 and pH 5.9 (Student's t test, p value < 0.05), and the oxalate biodegradation rate significantly at pH 5.9 (Student's t test, p value < 0.05).

Deleted: ¶

Deleted: carboxylic

Deleted: carboxylic

Deleted: carboxylic

Deleted: decreases

Formatted: Font: Italic

Deleted: carboxylic

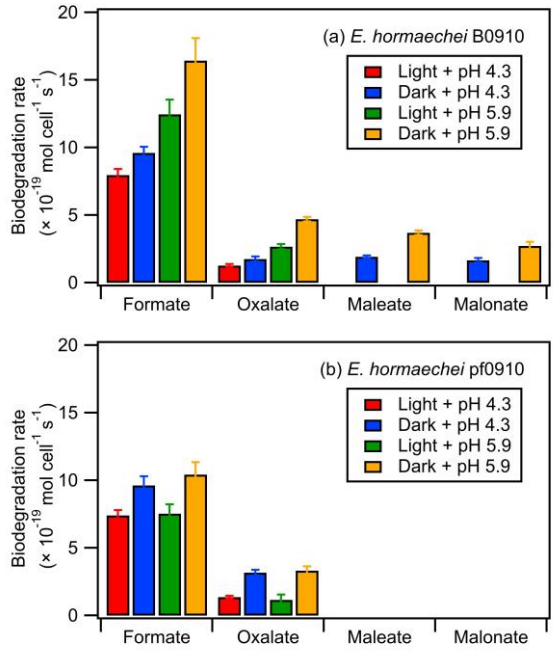

Figure 4. Biodegradation rates of oxalate, maleate, and malonate by (a) *E. hormaechei* B0910 and (b) *E. hormaechei* pf0910 under light and dark conditions at pH 4.3 and pH 5.9. Error bars represent one standard deviation from the mean biodegradation rate.

The survival rates and ADP/ATP ratios of both strains were also monitored during the biodegradation experiments (Figure S13). There were no significant changes in the survival rates and ADP/ATP ratios of both strains during the biodegradation process under dark conditions at pH 4.3, as well as under dark and illuminated conditions at pH 5.9. In contrast, the concentrations of viable cells gradually decreased until only 48% and 60% of the initial concentrations of viable cells remained at 12 h for *E. hormaechei* B0910 and *E. hormaechei* pf0910, respectively, during exposure to light at pH 4.3. The ADP/ATP ratios for both strains also increased during this time period, consistent with the lower metabolic activity and lower survival rate.

A simple kinetic analysis was performed to identify the factors that will impact the relative contributions of bacterial activity vs. ·OH/NO_3· chemistry in cloud water during the daytime and nighttime. Details of the calculations performed in this kinetic analysis can be found in Section S5. Our approach of considering daytime and nighttime processes separately was different from the approach used by previous studies, which determined the relative contributions of bacterial activity and chemical reactions on the degradation of organic compounds by only considering dark biodegradation processes and ·OH photochemical reactions (Vaïtilingom et al., 2011; Jaber et al., 2020; Jaber et al., 2021). Here, biodegradation rates that were measured under illuminated conditions were used for the daytime scenario, while biodegradation rates that were measured under dark conditions were used for the nighttime scenario. We used the average of biodegradation rates measured for the two strains for our calculations. Formate, oxalate, and malonate were chosen for our analysis since their ·OH and NO_3· reaction rate constants were available in the literature. ·OH and NO_3· are the main tropospheric aqueous-phase free radicals during the daytime and nighttime, respectively (Herrmann et al., 2010). The average measured biodegradation rates of formate, oxalate, and malonate were first converted to biodegradation rate constants. These biodegradation rate constants and the corresponding ·OH and NO_3· reaction rate constants provided by the literature (Table 1) were subsequently used for calculations of the biodegradation rates and chemical reaction rates in cloud water (Section S5). A bacteria concentration of 8×10^7 cell L^{-1} was assumed in our calculations for the daytime scenario at pH ~5 and the nighttime scenarios at pH ~4 and ~5, which was the same bacteria concentration used in previous studies and represented the highest estimate of actual live bacteria concentrations (i.e., 100% of metabolically active cells) (Vaïtilingom et al., 2011; Jaber et al., 2020; Jaber et al., 2021). Based on our investigations of the survival and energetic metabolism of bacteria under illuminated conditions at pH 4 to 5 (Figure 1), we expect the bacteria concentrations to gradually decrease for the daytime scenario at pH ~4. Thus, for simplicity, we assumed a lower bacteria concentration in our calculations for the daytime scenario at pH ~4, whereby we multiplied the bacteria concentration of 8×10^7 cell L^{-1} by a factor of 0.75. This factor was obtained by taking the average survival rates for the two strains from reaction time 0 to 12 hour in our experiments conducted under illuminated conditions at pH 4.3 (Figure S13). The rates of oxidation by ·OH

Deleted: determine

Deleted: whether the measured biodegradation rates are competitive with aqueous-phase chemical reactions in transforming carboxylicorganic acids

Deleted: S6

Deleted: constant

and NO_3· chemical reactions will depend on their respective concentrations. Hence, we used the average ·OH and NO_3· concentrations reported by Herrmann et al. (2010) for remote, marine, and urban environments in our calculations (Table S6) (Herrmann et al., 2010).

Deleted: S5

Table 1. Rate constants used to estimate the loss rates by biodegradation and chemical reactions (i.e., ·OH oxidation (daytime) and NO_3· (nighttime)).

Rate constant (Daytime)				
Reaction		Formic	Oxalic	Reference
Chemical	$k_{OH,Acid}$ $(L\ mol^{-1}\ s^{-1})$	2.40×10^{9}	1.60×10^{8}	(Ervens et al., 2003)
Biodegradation	$k_{cell,acid}$ (pH ~4) $(L\ cell^{-1} s^{-1})$	1.53×10^{-13}	2.65×10^{-15}	This study
	$k_{cell,acid}$ (pH ~5) $(L\ cell^{-1} s^{-1})$	1.92×10^{-13}	2.36×10^{-14}	This study

Rate constant (Nighttime)					
Reaction		Formate	Oxalate	Malonate	Reference
Chemical	$k_{NO_3,Acid}$ $(L\ mol^{-1}\ s^{-1})$	4.20×10^{7}	4.40×10^{7}	5.60×10^{6}	(Herrmann et al., 2010)
Biodegradation	$k_{cell,acid}$ (pH ~4) $(L\ cell^{-1} s^{-1})$	1.92×10^{-13}	5.18×10^{-15}	2.81×10^{-15}	This study
	$k_{cell,acid}$ (pH ~5) $(L\ cell^{-1} s^{-1})$	2.59×10^{-13}	7.80×10^{-14}	4.55×10^{-14}	This study

Calculations were performed for a variety of remote, marine, and urban environments with different formate, oxalate, and malonate concentrations that were previously reported in the literature (Table S7). Figure 5 shows the predicted relative contributions of bacterial activity vs. ·OH/NO_3· chemistry in remote, marine, and urban environments. ·OH photochemistry will make a larger contribution to the daytime degradation of formate and oxalate in remote and marine environments due to the high ·OH concentrations in these environments (2.2×10^{-14} M and 2×10^{-12} M, respectively). In contrast, bacterial activity will play a bigger role in the daytime degradation of formate in urban environments due to their lower ·OH concentrations (3.5×10^{-15} M). However, ·OH photochemistry will play a larger role in the daytime degradation of oxalate in urban environments due to the slow oxalate biodegradation rates. The low nighttime NO_3· concentrations in remote and marine

Deleted: S6

environments (5.1×10^{-15} M and 6.9×10^{-15} M, respectively) will result in bacterial activity playing a bigger role in the nighttime degradation of formate, oxalate, and malonate in these two environments. In urban environments, bacterial activity will play a bigger role in the nighttime degradation of formate, but the nighttime degradation of oxalate and malonate will be dominated by $NO_3\cdot$ chemistry due to the slow biodegradation rates of oxalate and malonate.

Our simple kinetic analysis indicated that the organic acid, cloud water pH, radical oxidant concentration, and time of day (i.e., daytime vs. nighttime) will impact the relative contributions of bacterial activity vs. $\cdot OH/NO_3\cdot$ chemistry in the aqueous phase. However, there are a number of caveats that should be noted. First, the biodegradation rates used in this analysis were from experiments conducted at 25 °C, which may be more representative of warmer regions during the summer (e.g., Hong Kong and parts of South China). Slower biodegradation rates will likely be measured at lower temperatures (Ariya et al., 2002; Vaitilingom et al., 2010; Husárová et al., 2011; Vaïtilingom et al., 2011), which will impact the relative contributions of bacterial activity vs. $\cdot OH/NO_3\cdot$ chemistry. Second, our analysis did not account for how the presence of aqueous-phase oxidants (e.g., $\cdot OH$ in the daytime, $NO_3\cdot$ in the nighttime) will impact the survival and energetic metabolism of bacteria, which in turn will impact the relative contributions of bacterial activity vs. $\cdot OH/NO_3\cdot$ chemistry. Third, our analysis did not account for the physical separation of cloud droplets containing bacteria cells from cell-free cloud droplets. Only a small fraction of cloud droplets will contain metabolically active bacteria cells, and the bacterial metabolism cannot affect the composition of organic acids in cell-free cloud droplets (Fankhauser et al., 2019; Khaled et al., 2021). Hence, only $\cdot OH/NO_3\cdot$ chemistry will govern the degradation of organic acids in cell-free droplets. Consequently, not accounting for the physical separation of cloud droplets containing bacteria cells from cell-free cloud droplets will result in an overestimation of the overall contribution of bacterial activity to the biodegradation of organic compounds (Fankhauser et al., 2019; Khaled et al., 2021). Fourth, our analysis only considers biodegradation and chemical reactions occurring in the aqueous phase and ignores gas-aqueous phase exchanges and gas-phase chemical reactions. Nah et al. (2018) previously showed that the gas-aqueous phase partitioning of organic acids will depend on the organic acid's Henry's law constant and acid

Deleted: verall, o

Deleted: the measured biodegradation rates can be competitive with aqueous-phase chemical reactions in transforming carboxylicorganic acids in cloud water, but it will depend on

Deleted: carboxylic

dissociation constants, liquid water concentration, temperature, and pH (Section S6). Figure S14 shows that a significant fraction of formic acid will be in the gas phase at pH 4 and 5 under cloud water conditions, whereas all of oxalic acid, malonic acid, and maleic acid will be in the aqueous phase at pH 4 and 5 under cloud water conditions. This suggests that gas-phase chemical reactions will likely play an important role in consuming formic acid, whereas the consumption of oxalic acid, malonic acid, and maleic acid will likely mainly be through bacterial activity and chemical reactions in the aqueous phase. Quantifying the exact contributions of aqueous-phase bacterial activity vs. aqueous-phase $\cdot OH/NO_3\cdot$ chemistry vs. gas-phase $\cdot OH/NO_3\cdot$ chemistry under different cloud water pH conditions will require a multi-phase box model similar to the one used by Khaled et al. (2021). This is beyond the scope of the current study but can be a subject of future studies.

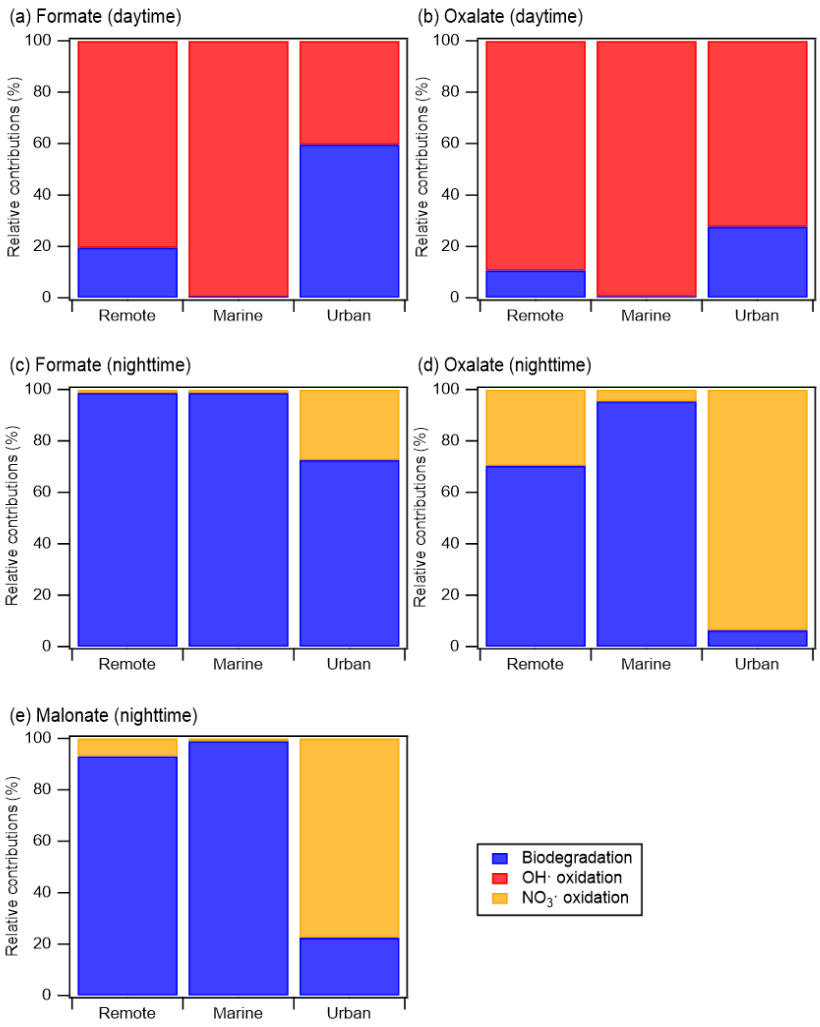

711

712 **Figure 5.** Predicted relative contributions of bacterial activity and chemical reaction (i.e., ·OH

713 oxidation (daytime) and NO_3· (nighttime)) to the degradation of organic compounds in the

714 aqueous phase in remote, marine, and urban areas. This figure is based on estimated loss rates

715 shown in Table S7.

716 **4. Summary and implications**

Deleted: carboxylic

Deleted: S6

Deleted: ¶

Deleted: **Conclusions**

In this study, we investigated how cloud water pH and exposure to solar radiation impact the survival and energetic metabolism of bacteria and their ability to biodegrade organic acids in clouds. Laboratory experiments were performed using artificial solar radiation and artificial cloud water that mimicked the pH and composition of cloud water previously collected in South China, which is a region with fairly acidic cloud water (pH 3 to 5.9). Using two *E. hormaechei* strains that were isolated from ambient air in Hong Kong, we observed that the energetic metabolism and survival of both strains depended on the artificial cloud water pH. Low survival rates were observed for both strains at pH < 4 regardless whether the strains were exposed to light. At pH 4 to 5, the energetic metabolism and survival of both strains were only negatively impacted when they were exposed to light. In contrast, there were minimal effects on the energetic metabolism and survival of both strains when they were exposed to simulated sunlight at pH > 5. In addition, the biodegradation of organic acids depended on the presence (or absence) of light and the artificial cloud water pH. The measured biodegradation rates were around 10^{-19} to 10^{-18} mol cell^{-1} s^{-1}, which were on the same order of magnitude as the bacterial strains isolated from cloud water and implemented into cloud models (Vaitilingom et al., 2010; Vaïtilingom et al., 2011; Fankhauser et al., 2019). Our analysis indicated that the organic acid, cloud water pH, radical oxidant concentration, and the time of day will impact the relative contributions of bacterial activity vs. ·OH/NO_3· chemistry in the aqueous phase.

This study has two important implications for our understanding of bacteria in clouds. First, this study underscores the importance of accounting for cloud water pH when simulating cloud processes involving metabolically active bacteria in atmospheric models, including microbiological-chemical interactions between live bacteria and organic matter. Results from this study imply the cloud water pH will impact the bacteria's ability to survive and thrive in during the daytime and/or nighttime. The pH of cloud water typically lies between 3 and 6 (Pye et al., 2020). Regions with high inputs of sulfuric acid and/or nitric acid combined with low inputs of ammonia, dust, and sea salt, such as South China, will have moderately acidic to highly acidic cloud water (Li et al., 2020; Pye et al., 2020; Shah et al., 2020; Qu and Han, 2021). Most of the bacteria in the atmosphere are neutrophiles that generally survive and thrive in less acidic environments. Hence, even though our study focuses on two *Enterobacter* strains,

Deleted: carboxylic

Deleted: an aerosol sample

Deleted: carboxylic

Deleted: carboxylic

Deleted: determine whether the measured biodegradation rates will

Deleted: be competitive with aqueous-phase chemical reactions in transforming carboxylicorganic acids in cloud water…

Deleted: that there is a minimum

Deleted: threshold at which

Deleted: will

762 we hypothesize that cloud water pH will also affect the ability of other neutrophilic bacteria
763 species to survive and remain metabolically active. Second, results from this study imply that
764 it is important to consider the potential synergistic negative impacts that different stressors have
765 on the survival and microbial activity of bacteria in clouds. Much of our current knowledge on
766 the effect of different stressors (osmotic shocks, freeze-thaw cycles, and exposure to light and
767 H_2O_2) on the survival of bacteria in clouds originate from a previous study by Joly et al. (2015)
768 who investigated the impacts of these four stressors individually. However, as demonstrated in
769 this study, when combined together, some stressors (in this case, cloud water pH and exposure
770 to sunlight) can have synergistic negative impacts on the survival and microbial activity of
771 bacteria in clouds.

772 While this study builds on our existing knowledge of how different stressors will impact
773 the survival and energetic metabolism of bacteria and their ability to biodegrade organic matter
774 in clouds, there are a number of caveats that should be noted. First, we were limited to using
775 bacterial strains isolated from ambient air in this study due to the unavailability of bacteria
776 isolates from cloud water in South China. Thus, if available, this work could be extended to
777 bacteria isolates from cloud water in South China in the future to determine the pH conditions
778 at which these isolates can survive and participate in microbiological-chemical interactions
779 during the daytime and/or nighttime. The effect of cloud water pH on bacteria species that are
780 reportedly common in cloud water (e.g., *Sphingomonadales*, *Rhodospirillales*, *Rhizobiales*,
781 *Burkholderiales*, *Pseudomonadales* (Vaïtilingom et al., 2012; Zhu et al., 2018; Peng et al.,
782 2019)) should also be investigated. Second, all the experiments in this study were conducted at
783 25 °C, which may be more representative of warmer regions during the summer (e.g., Hong
784 Kong and parts of South China). Several studies have reported slower biodegradation rates at
785 lower temperatures (Ariya et al., 2002; Vaitilingom et al., 2010; Husárová et al., 2011;
786 Vaïtilingom et al., 2011), which suggest that cloud water temperature may influence the
787 survival and energetic metabolism of bacteria. Third, the photon intensity in the photoreactor
788 was kept constant in all the experiments. However, sunlight intensity will change throughout
789 the day in the atmosphere. Fourth, this study does not consider how the presence of aqueous-
790 phase oxidants (e.g., ·OH in the daytime, NO_3· in the nighttime) will impact the survival and

Deleted: an aerosol sample

energetic metabolism of bacteria in clouds. Hence, the effects of temperature, light intensity, and oxidants on the impact the survival and energetic metabolism of bacteria and their ability to biodegrade organic matter in clouds should be investigated in future studies.

Data availability: The data used in this publication is available to the community and can be accessed on request to the corresponding author (theodora.nah@cityu.edu.hk), or at: https://doi.org/10.5281/zenodo.7045510 (Liu et al., 2022).

Author contributions: Y.L., P.L., and T.N. designed the study. Y.L. conducted the experiments. Y.L., C.K.L., and Z.S. performed the data analysis. Y.L. and T.N. wrote the manuscript with contributions from all co-authors.

Competing interests: One of the authors is a member of the editorial board of *Atmospheric Chemistry and Physics*. The peer-review process was guided by an independent editor, and the authors also have no other competing interests to declare.

Acknowledgements: This work was supported by the National Natural Science Foundation of China (project number R-BTC7801) and the Research Grants Council of Hong Kong (project number 11303720).

References

Amato, P., Besaury, L., Joly, M., Penaud, B., Deguillaume, L., and Delort, A.-M.: Metatranscriptomic exploration of microbial functioning in clouds, Scientific Reports, 9, 1-12, 2019.

Amato, P., Ménager, M., Sancelme, M., Laj, P., Mailhot, G., and Delort, A.-M.: Microbial population in cloud water at the Puy de Dôme: Implications for the chemistry of clouds, Atmospheric Environment, 39, 4143-4153, https://doi.org/10.1016/j.atmosenv.2005.04.002, 2005.

Amato, P., Parazols, M., Sancelme, M., Mailhot, G., Laj, P., and Delort, A.-M.: An important oceanic source of micro-organisms for cloud water at the Puy de Dôme (France), Atmospheric Environment, 41, 8253-8263, https://doi.org/10.1016/j.atmosenv.2007.06.022, 2007.

Amato, P., Joly, M., Besaury, L., Oudart, A., Taib, N., Mone, A. I., Deguillaume, L., Delort, A. M., and Debroas, D.: Active microorganisms thrive among extremely diverse communities in cloud water, PLoS One, 12, e0182869, https://doi.org/10.1371/journal.pone.0182869, 2017.

Anglada, J. M., Martins-Costa, M., Francisco, J. S., and Ruiz-Lopez, M. F.: Interconnection of reactive oxygen species chemistry across the interfaces of atmospheric, environmental, and biological processes, Accounts of chemical research, 48, 575-583, https://doi.org/10.1021/ar500412p, 2015.

Ariya, P. A., Nepotchatykh, O., Ignatova, O., and Amyot, M.: Microbiological degradation of atmospheric organic compounds, Geophysical Research Letters, 29, 34-31-34-34, https://doi.org/10.1029/2002gl015637, 2002.

Attard, E., Yang, H., Delort, A. M., Amato, P., Pöschl, U., Glaux, C., Koop, T., and Morris, C. E.: Effects of atmospheric conditions on ice nucleation activity of Pseudomonas, Atmospheric Chemistry and Physics, 12, 10667-10677, https://doi.org/10.5194/acp-12-10667-2012, 2012.

Bauer, H., Kasper-Giebl, A., Loflund, M., Giebl, H., Hitzenberger, R., Zibuschka, F., and Puxbaum, H.: The contribution of bacteria and fungal spores to the organic carbon content of cloud water, precipitation and aerosols, Atmospheric Research, 64, 109-119, https://doi.org/10.1016/s0169-8095(02)00084-4, 2002.

Bearson, S., Bearson, B., and Foster, J. W.: Acid stress responses in enterobacteria, Fems Microbiology Letters, 147, 173-180, https://doi.org/10.1111/j.1574-6968.1997.tb10238.x, 1997.

Bianco, A., Voyard, G., Deguillaume, L., Mailhot, G., and Brigante, M.: Improving the characterization of dissolved organic carbon in cloud water: Amino acids and their impact on the oxidant capacity, Sci Rep, 6, 37420, https://doi.org/10.1038/srep37420, 2016.

Bianco, A., Deguillaume, L., Chaumerliac, N., Vaïtilingom, M., Wang, M., Delort, A.-M., and Bridoux, M. C.: Effect of endogenous microbiota on the molecular composition of cloud water: a study by Fourier-transform ion cyclotron resonance mass spectrometry (FT-ICR MS), Scientific Reports, 9, 7663, https://doi.org/10.1038/s41598-019-44149-8, 2019.

Bianco, A., Deguillaume, L., Vaitilingom, M., Nicol, E., Baray, J. L., Chaumerliac, N., and Bridoux, M.: Molecular Characterization of Cloud Water Samples Collected at the Puy de Dome (France) by Fourier Transform Ion Cyclotron Resonance Mass Spectrometry, Environmental Science & Technology, 52, 10275-10285, https://doi.org/10.1021/acs.est.8b01964, 2018.

Brzoska, R. M., Edelmann, R. E., and Bollmann, A.: Physiological and Genomic Characterization of Two Novel Bacteroidota Strains Asinibacterium spp. OR43 and OR53, Bacteria, 1, 33-47, 2022.

Burrell, M. R., Just, V. J., Bowater, L., Fairhurst, S. A., Requena, L., Lawson, D. M., and Bornemann, S.: Oxalate decarboxylase and oxalate oxidase activities can be interchanged with a specificity switch of up to 282 000 by mutating an active site lid, Biochemistry, 46, 12327-12336, https://doi.org/10.1021/bi700947s, 2007.

Burrows, S. M., Elbert, W., Lawrence, M. G., and Poschl, U.: Bacteria in the global atmosphere

- Part 1: Review and synthesis of literature data for different ecosystems, Atmospheric Chemistry and Physics, 9, 9263-9280, https://doi.org/10.5194/acp-9-9263-2009, 2009.

Chen, X., Ran, P., Ho, K., Lu, W., Li, B., Gu, Z., Song, C., and Wang, J.: Concentrations and Size Distributions of Airborne Microorganisms in Guangzhou during Summer, Aerosol and Air Quality Research, 12, 1336-1344, https://doi.org/10.4209/aaqr.2012.03.0066, 2012.

Davey, M. E. and O'toole, G. A.: Microbial biofilms: from ecology to molecular genetics, Microbiology and molecular biology reviews, 64, 847-867, https://doi.org/10.1128/MMBR.64.4.847-867.2000, 2000.

Delort, A.-M., Vaïtilingom, M., Amato, P., Sancelme, M., Parazols, M., Mailhot, G., Laj, P., and Deguillaume, L.: A short overview of the microbial population in clouds: Potential roles in atmospheric chemistry and nucleation processes, Atmospheric Research, 98, 249-260, https://doi.org/10.1016/j.atmosres.2010.07.004, 2010.

Després, V., Huffman, J. A., Burrows, S. M., Hoose, C., Safatov, A., Buryak, G., Fröhlich-Nowoisky, J., Elbert, W., Andreae, M., Pöschl, U., and Jaenicke, R.: Primary biological aerosol particles in the atmosphere: a review, Tellus B: Chemical and Physical Meteorology, 64, https://doi.org/10.3402/tellusb.v64i0.15598, 2012.

Ding, W., Li, L., Han, Y., Liu, J., and Liu, J.: Site-related and seasonal variation of bioaerosol emission in an indoor wastewater treatment station: level, characteristics of particle size, and microbial structure, Aerobiologia, 32, 211-224, https://doi.org/10.1007/s10453-015-9391-5, 2015.

Eichhorn, E. and Leisinger, T.: Escherichia coli utilizes methanesulfonate and L-cysteate as sole sulfur sources for growth, FEMS microbiology letters, 205, 271-275, https://doi.org/10.1111/j.1574-6968.2001.tb10960.x, 2001.

Ervens, B. and Amato, P.: The global impact of bacterial processes on carbon mass, Atmospheric Chemistry and Physics, 20, 1777-1794, https://doi.org/10.5194/acp-20-1777-2020, 2020.

Ervens, B., Gligorovski, S., and Herrmann, H.: Temperature-dependent rate constants for hydroxyl radical reactions with organic compounds in aqueous solutions, Physical Chemistry Chemical Physics, 5, 1811-1824, https://doi.org/10.1039/B300072A, 2003.

Fankhauser, A. M., Antonio, D. D., Krell, A., Alston, S. J., Banta, S., and McNeill, V. F.: Constraining the Impact of Bacteria on the Aqueous Atmospheric Chemistry of Small Organic Compounds, ACS Earth and Space Chemistry, 3, 1485-1491, https://doi.org/10.1021/acsearthspacechem.9b00054, 2019.

Flemming, H. C. and Wingender, J.: The biofilm matrix, Nature Reviews Microbiology, 8, 623-633, https://doi.org/10.1038/nrmicro2415, 2010.

George, K. M., Ruthenburg, T. C., Smith, J., Yu, L., Zhang, Q., Anastasio, C., and Dillner, A.

M.: FT-IR quantification of the carbonyl functional group in aqueous-phase secondary organic aerosol from phenols, Atmospheric Environment, 100, 230-237, https://doi.org/10.1016/j.atmosenv.2014.11.011, 2015.

Gimenez, R., Nuñez, M. F., Badia, J., Aguilar, J., and Baldoma, L.: The gene yjcG, cotranscribed with the gene acs, encodes an acetate permease in Escherichia coli, Journal of bacteriology, 185, 6448-6455, https://doi.org/10.1128/JB.185.21.6448-6455.2003, 2003.

Guan, N. and Liu, L.: Microbial response to acid stress: mechanisms and applications, Applied Microbiology and Biotechnology, 104, 51-65, https://doi.org/10.1007/s00253-019-10226-1, 2020.

Hatakeyama, K., GoTo, M., Kobayashi, M., Terasawa, M., and Yukawa, H.: Analysis of oxidation sensitivity of maleate cis-trans isomerase from Serratia marcescens, Bioscience, biotechnology, and biochemistry, 64, 1477-1485, https://doi.org/10.1271/bbb.64.1477, 2000.

Herrmann, H., Hoffmann, D., Schaefer, T., Brauer, P., and Tilgner, A.: Tropospheric aqueous-phase free-radical chemistry: radical sources, spectra, reaction kinetics and prediction tools, Chemphyschem, 11, 3796-3822, https://doi.org/10.1002/cphc.201000533, 2010.

Hu, W., Niu, H. Y., Murata, K., Wu, Z. J., Hu, M., Kojima, T., and Zhang, D. Z.: Bacteria in atmospheric waters: Detection, characteristics and implications, Atmospheric Environment, 179, 201-221, https://doi.org/10.1016/j.atmosenv.2018.02.026, 2018.

Huang, D. D., Zhang, Q., Cheung, H. H. Y., Yu, L., Zhou, S., Anastasio, C., Smith, J. D., and Chan, C. K.: Formation and Evolution of aqSOA from Aqueous-Phase Reactions of Phenolic Carbonyls: Comparison between Ammonium Sulfate and Ammonium Nitrate Solutions, Environmental Science & Technology, 52, 9215-9224, https://doi.org/10.1021/acs.est.8b03441, 2018.

Huang, S., Hu, W., Chen, J., Wu, Z., Zhang, D., and Fu, P.: Overview of biological ice nucleating particles in the atmosphere, Environment International, 146, 106197, https://doi.org/10.1016/j.envint.2020.106197, 2021.

Husárová, S., Vaïtilingom, M., Deguillaume, L., Traikia, M., Vinatier, V., Sancelme, M., Amato, P., Matulová, M., and Delort, A.-M.: Biotransformation of methanol and formaldehyde by bacteria isolated from clouds. Comparison with radical chemistry, Atmospheric Environment, 45, 6093-6102, https://doi.org/10.1016/j.atmosenv.2011.06.035, 2011.

Ichihara, A. and Ichihara, E. A.: Metabolism of L-Lysine by Bacterial Enzymes V. Glutaric Semialdehyde Dehydrogenase, The Journal of Biochemistry, 49, 154-157, https://doi.org/10.1093/oxfordjournals.jbchem.a127272, 1961.

Jaber, S., Joly, M., Brissy, M., Leremboure, M., Khaled, A., Ervens, B., and Delort, A.-M.: Biotic and abiotic transformation of amino acids in cloud water: experimental studies and atmospheric implications, Biogeosciences, 18, 1067-1080, https://doi.org/10.5194/bg-18-1067-2021, 2021.

Jaber, S., Lallement, A., Sancelme, M., Leremboure, M., Mailhot, G., Ervens, B., and Delort, A.-M.: Biodegradation of phenol and catechol in cloud water: comparison to chemical oxidation in the atmospheric multiphase system, Atmospheric Chemistry and Physics, 20, 4987-4997, https://doi.org/10.5194/acp-20-4987-2020, 2020.

Jaenicke, R.: Abundance of cellular material and proteins in the atmosphere, Science, 308, 73-73, https://doi.org/10.1126/science.1106335, 2005.

Joly, M., Amato, P., Sancelme, M., Vinatier, V., Abrantes, M., Deguillaume, L., and Delort, A.-M.: Survival of microbial isolates from clouds toward simulated atmospheric stress factors, Atmospheric Environment, 117, 92-98, https://doi.org/10.1016/j.atmosenv.2015.07.009, 2015.

Kahnert, A., Vermeij, P., Wietek, C., James, P., Leisinger, T., and Kertesz, M. A.: The ssu locus plays a key role in organosulfur metabolism in Pseudomonas putida S-313, Journal of bacteriology, 182, 2869-2878, https://doi.org/10.1128/JB.182.10.2869-2878.2000, 2000.

Kanehisa, M., Sato, Y., and Kawashima, M.: KEGG mapping tools for uncovering hidden features in biological data, Protein Science, 31, 47-53, https://doi.org/10.1002/pro.4172, 2022.

Kawamura, K., Ishimura, Y., and Yamazaki, K.: Four years' observations of terrestrial lipid class compounds in marine aerosols from the western North Pacific, Global Biogeochemical Cycles, 17, https://doi.org/10.1029/2001gb001810, 2003.

Khaled, A., Zhang, M., Amato, P., Delort, A.-M., and Ervens, B.: Biodegradation by bacteria in clouds: an underestimated sink for some organics in the atmospheric multiphase system, Atmospheric Chemistry and Physics, 21, 3123-3141, 2021.

Koutny, M., Sancelme, M., Dabin, C., Pichon, N., Delort, A.-M., and Lemaire, J.: Acquired biodegradability of polyethylenes containing pro-oxidant additives, Polymer Degradation and Stability, 91, 1495-1503, https://doi.org/10.1016/j.polymdegradstab.2005.10.007, 2006.

Krulwich, T. A., Sachs, G., and Padan, E.: Molecular aspects of bacterial pH sensing and homeostasis, Nature Reviews Microbiology, 9, 330-343, 2011.

Krumins, V., Mainelis, G., Kerkhof, L. J., and Fennell, D. E.: Substrate-dependent rRNA production in an airborne bacterium, Environmental Science & Technology Letters, 1, 376-381, 2014.

Laszakovits, J. R. and MacKay, A. A.: Data-Based Chemical Class Regions for Van Krevelen Diagrams, Journal of the American Society for Mass Spectrometry, 33, 198-202, https://doi.org/10.1021/jasms.1c00230, 2022.

Lee, A. K. Y., Chan, C. K., Fang, M., and Lau, A. P. S.: The 3-hydroxy fatty acids as biomarkers for quantification and characterization of endotoxins and Gram-negative bacteria in atmospheric aerosols in Hong Kong, Atmospheric Environment, 38, 6307-6317, https://doi.org/10.1016/j.atmosenv.2004.08.013, 2004.

966 Li, T., Wang, Z., Wang, Y., Wu, C., Liang, Y., Xia, M., Yu, C., Yun, H., Wang, W., Wang, Y.,
967 Guo, J., Herrmann, H., and Wang, T.: Chemical characteristics of cloud water and the impacts
968 on aerosol properties at a subtropical mountain site in Hong Kong SAR, Atmospheric
969 Chemistry and Physics, 20, 391-407, https://doi.org/10.5194/acp-20-391-2020, 2020.

970 Li, Y., He, Y., Lam, C. H., and Nah, T.: Environmental photochemistry of organic UV filter
971 butyl methoxydibenzoylmethane: Implications for photochemical fate in surface waters,
972 Science of The Total Environment, 839, 156145,
973 https://doi.org/10.1016/j.scitotenv.2022.156145, 2022.

974 Liu, K., Xu, Y., and Zhou, N.-Y.: Identification of a specific maleate hydratase in the direct
975 hydrolysis route of the gentisate pathway, Applied and Environmental Microbiology, 81, 5753-
976 5760, https://doi.org/10.1128/AEM.00975-15, 2015.

977 Liu, M., Devlin, J. C., Hu, J., Volkova, A., Battaglia, T. W., Ho, M., Asplin, J. R., Byrd, A., Li,
978 H., and Ruggles, K. V.: Microbial genetic and transcriptional contributions to oxalate
979 degradation by the gut microbiota in health and disease, Elife, 10, e63642,
980 https://doi.org/10.7554/eLife.63642, 2021.

981 Löflund, M., Kasper-Giebl, A., Schuster, B., Giebl, H., Hitzenberger, R., and Puxbaum, H.:
982 Formic, acetic, oxalic, malonic and succinic acid concentrations and their contribution to
983 organic carbon in cloud water, Atmospheric Environment, 36, 1553-1558,
984 https://doi.org/10.1016/S1352-2310(01)00573-8, 2002.

985 Lund, P., Tramonti, A., and De Biase, D.: Coping with low pH: molecular strategies in
986 neutralophilic bacteria, FEMS Microbiology Reviews, 38, 1091-1125,
987 https://doi.org/10.1111/1574-6976.12076, 2014.

988 Matulova, M., Husarova, S., Capek, P., Sancelme, M., and Delort, A. M.: Biotransformation of
989 various saccharides and production of exopolymeric substances by cloud-borne Bacillus sp.
990 3B6, Environ Sci Technol, 48, 14238-14247, https://doi.org/10.1021/es501350s, 2014.

991 Misovich, M. V., Hettiyadura, A. P. S., Jiang, W. Q., Zhang, Q., and Laskin, A.: Molecular-
992 Level Study of the Photo-Oxidation of Aqueous-Phase Guaiacyl Acetone in the Presence of C-
993 3*: Formation of Brown Carbon Products, Acs Earth and Space Chemistry, 5, 1983-1996,
994 https://doi.org/10.1021/acsearthspacechem.1c00103, 2021.

995 Möhler, O., DeMott, P., Vali, G., and Levin, Z.: Microbiology and atmospheric processes: the
996 role of biological particles in cloud physics, Biogeosciences, 4, 1059-1071,
997 https://doi.org/10.5194/bg-4-1059-2007, 2007.

998 Morris, C. E., Soubeyrand, S., Bigg, E. K., Creamean, J. M., and Sands, D. C.: Mapping
999 Rainfall Feedback to Reveal the Potential Sensitivity of Precipitation to Biological Aerosols,
1000 Bulletin of the American Meteorological Society, 98, 1109-1118,
1001 https://doi.org/10.1175/BAMS-D-15-00293.1, 2017.

1002 Morris, C. E., Conen, F., Alex Huffman, J., Phillips, V., Pöschl, U., and Sands, D. C.:

Bioprecipitation: a feedback cycle linking earth history, ecosystem dynamics and land use through biological ice nucleators in the atmosphere, Glob Chang Biol, 20, 341-351, https://doi.org/10.1111/gcb.12447, 2014.

Nah, T., Guo, H., Sullivan, A. P., Chen, Y., Tanner, D. J., Nenes, A., Russell, A., Ng, N. L., Huey, L. G., and Weber, R. J.: Characterization of aerosol composition, aerosol acidity, and organic acid partitioning at an agriculturally intensive rural southeastern US site, Atmos. Chem. Phys., 18, 11471-11491, https://doi.org/10.5194/acp-18-11471-2018, 2018.

Péguilhan, R., Besaury, L., Rossi, F., Enault, F., Baray, J.-L., Deguillaume, L., and Amato, P.: Rainfalls sprinkle cloud bacterial diversity while scavenging biomass, FEMS Microbiology Ecology, 97, https://doi.org/10.1093/femsec/fiab144, 2021.

Peng, J., Zhou, S., Xiao, K., Zeng, J., Yao, C., Lu, S., Zhang, W., Fu, Y., Yang, Y., and Bi, X.: Diversity of bacteria in cloud water collected at a National Atmospheric Monitoring Station in Southern China, Atmospheric Research, 218, 176-182, https://doi.org/10.1016/j.atmosres.2018.12.004, 2019.

Prokof'eva, T. V., Shoba, S. A., Lysak, L. V., Ivanova, A. E., Glushakova, A. M., Shishkov, V. A., Lapygina, E. V., Shilaika, P. D., and Glebova, A. A.: Organic Constituents and Biota in the Urban Atmospheric Solid Aerosol: Potential Effects on Urban Soils, Eurasian Soil Science, 54, 1532-1545, https://doi.org/10.1134/S1064229321100094, 2021.

Pye, H. O., Nenes, A., Alexander, B., Ault, A. P., Barth, M. C., Clegg, S. L., Collett Jr, J. L., Fahey, K. M., Hennigan, C. J., and Herrmann, H.: The acidity of atmospheric particles and clouds, Atmospheric chemistry and physics, 20, 4809-4888, https://doi.org/10.5194/acp-20-4809-2020, 2020.

Qu, R. and Han, G.: A critical review of the variation in rainwater acidity in 24 Chinese cities during 1982–2018, Elementa: Science of the Anthropocene, 9, https://doi.org/10.1525/elementa.2021.00142, 2021.

Rivas-Ubach, A., Liu, Y., Bianchi, T. S., Tolic, N., Jansson, C., and Pasa-Tolic, L.: Moving beyond the van Krevelen diagram: A new stoichiometric approach for compound classification in organisms, Analytical chemistry, 90, 6152-6160, 2018.

Romano, S., Fragola, M., Alifano, P., Perrone, M. R., and Talà, A.: Potential Human and Plant Pathogenic Species in Airborne PM10 Samples and Relationships with Chemical Components and Meteorological Parameters, Atmosphere, 12, 654, https://doi.org/10.3390/atmos12050654, 2021.

Romano, S., Di Salvo, M., Rispoli, G., Alifano, P., Perrone, M. R., and Tala, A.: Airborne bacteria in the Central Mediterranean: Structure and role of meteorology and air mass transport, Sci Total Environ, 697, 134020, https://doi.org/10.1016/j.scitotenv.2019.134020, 2019.

Ruiz-Gil, T., Acuña, J. J., Fujiyoshi, S., Tanaka, D., Noda, J., Maruyama, F., and Jorquera, M. A.: Airborne bacterial communities of outdoor environments and their associated influencing

factors, Environment International, 145, 106156, https://doi.org/10.1016/j.envint.2020.106156, 2020.

Sá-Pessoa, J., Paiva, S., Ribas, D., Silva, I. J., Viegas, S. C., Arraiano, C. M., and Casal, M.: SATP (YaaH), a succinate–acetate transporter protein in Escherichia coli, Biochemical journal, 454, 585-595, https://doi.org/10.1042/BJ20130412, 2013.

Shah, V., Jacob, D. J., Moch, J. M., Wang, X., and Zhai, S.: Global modeling of cloud water acidity, precipitation acidity, and acid inputs to ecosystems, Atmos. Chem. Phys., 20, 12223-12245, https://doi.org/10.5194/acp-20-12223-2020, 2020.

Sun, X., Wang, Y., Li, H., Yang, X., Sun, L., Wang, X., Wang, T., and Wang, W.: Organic acids in cloud water and rainwater at a mountain site in acid rain areas of South China, Environ Sci Pollut Res Int, 23, 9529-9539, https://doi.org/10.1007/s11356-016-6038-1, 2016.

Tsai, Y. I. and Kuo, S.-C.: Contributions of low molecular weight carboxylic acids to aerosols and wet deposition in a natural subtropical broad-leaved forest environment, Atmospheric Environment, 81, 270-279, https://doi.org/10.1016/j.atmosenv.2013.08.061, 2013.

Tyagi, P., Ishimura, Y., and Kawamura, K.: Hydroxy fatty acids in marine aerosols as microbial tracers: 4-year study on β-and ω-hydroxy fatty acids from remote Chichijima Island in the western North Pacific, Atmospheric Environment, 115, 89-100, 2015.

Vaitilingom, M., Amato, P., Sancelme, M., Laj, P., Leriche, M., and Delort, A. M.: Contribution of microbial activity to carbon chemistry in clouds, Appl Environ Microbiol, 76, 23-29, https://doi.org/10.1128/AEM.01127-09, 2010.

Vaitilingom, M., Deguillaume, L., Vinatier, V., Sancelme, M., Amato, P., Chaumerliac, N., and Delort, A. M.: Potential impact of microbial activity on the oxidant capacity and organic carbon budget in clouds, Proc Natl Acad Sci U S A, 110, 559-564, https://doi.org/10.1073/pnas.1205743110, 2013.

Vaïtilingom, M., Attard, E., Gaiani, N., Sancelme, M., Deguillaume, L., Flossmann, A. I., Amato, P., and Delort, A.-M.: Long-term features of cloud microbiology at the puy de Dôme (France), Atmospheric Environment, 56, 88-100, https://doi.org/10.1016/j.atmosenv.2012.03.072, 2012.

Vaïtilingom, M., Charbouillot, T., Deguillaume, L., Maisonobe, R., Parazols, M., Amato, P., Sancelme, M., and Delort, A. M.: Atmospheric chemistry of carboxylic acids: microbial implication versus photochemistry, Atmospheric Chemistry and Physics, 11, 8721-8733, https://doi.org/10.5194/acp-11-8721-2011, 2011.

Watson, J., Baker, T., and Bell, S.: Molecular biology of the gene, 6th edn. W, 2007.

Wei, M., Xu, C., Chen, J., Zhu, C., Li, J., and Lv, G.: Characteristics of bacterial community in cloud water at Mt Tai: similarity and disparity under polluted and non-polluted cloud episodes, Atmos. Chem. Phys., 17, 5253-5270, https://doi.org/10.5194/acp-17-5253-2017, 2017.

1076 Zhang, M., Khaled, A., Amato, P., Delort, A. M., and Ervens, B.: Sensitivities to biological
1077 aerosol particle properties and ageing processes: potential implications for aerosol–cloud
1078 interactions and optical properties, Atmos. Chem. Phys., 21, 3699-3724,
1079 https://doi.org/10.5194/acp-21-3699-2021, 2021.

1080 Zhou, H., Wang, X., Li, Z., Kuang, Y., Mao, D., and Luo, Y.: Occurrence and Distribution of
1081 Urban Dust-Associated Bacterial Antibiotic Resistance in Northern China, Environmental
1082 Science & Technology Letters, 5, 50-55, https://doi.org/10.1021/acs.estlett.7b00571, 2018.

1083 Zhu, C., Chen, J., Wang, X., Li, J., Wei, M., Xu, C., Xu, X., Ding, A., and Collett, J. L.:
1084 Chemical Composition and Bacterial Community in Size-Resolved Cloud Water at the Summit
1085 of Mt. Tai, China, Aerosol and Air Quality Research, 18, 1-14,
1086 https://doi.org/10.4209/aaqr.2016.11.0493, 2018.

1087

Supplementary Information

Effects of pH and light exposure on the survival of bacteria and their ability to biodegrade organic compounds in clouds: Implications for microbial activity in acidic cloud water

Yushuo Liu,[1,2] Chee Kent Lim,[1] Zhiyong Shen,[1] Patrick K. H. Lee,[1,3] Theodora Nah[1,2,3*]

[1]*School of Energy and Environment, City University of Hong Kong, Hong Kong SAR, China*
[2]*Shenzhen Research Institute, Nanshan District, Shenzhen, China*
[3]*State Key Laboratory of Marine Pollution, City University of Hong Kong, Hong Kong SAR, China*

** To whom correspondence should be addressed: Theodora Nah (Email: theodora.nah@cityu.edu.hk, Tel: +852 3442 5578)*

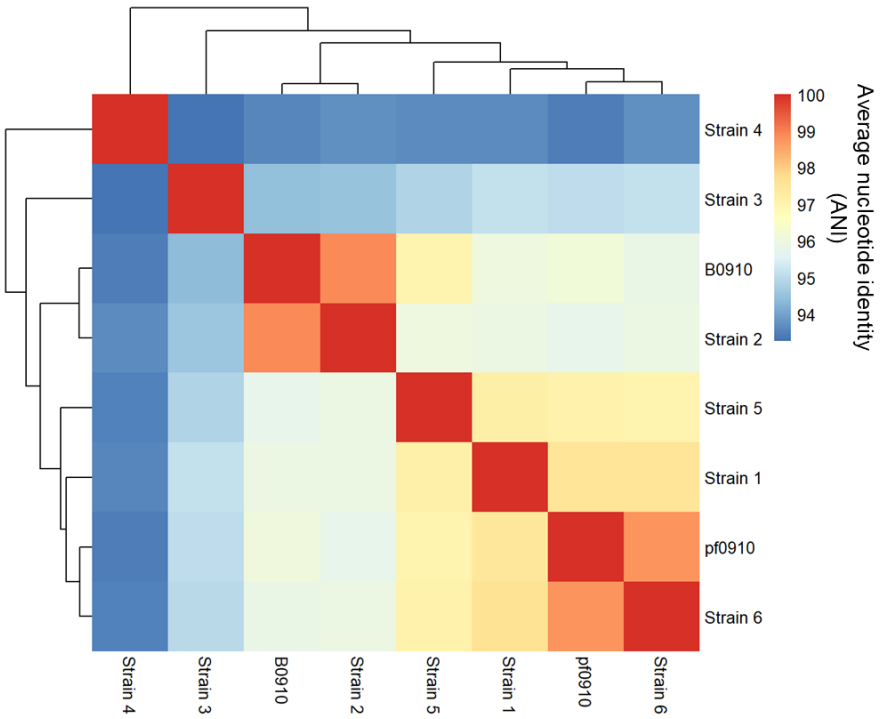

Figure S1. Average nucleotide identity (ANI) value of *Enterobacter* strains B00910, pf0910, and six others. **Strain 1:** *Enterobacter hormaechei* subsp. *oharae* DSM 16687; **Strain 2:** *Enterobacter hormaechei* subsp.hoffmannii DSM 14563; **Strain 3:** *Enterobacter hormaechei* ATCC 49162; **Strain 4**: *Enterobacter quasihormaechei*. GCF 004331385.1; **Strain 5:** *Enterobacter xiangfangensis* LMG27195; **Strain 6:** *Enterobacter hormaechei* subsp. *steigerwaltii* DSM 16691. Strains 1 to 6 are the closest identified neighbors with strains B0910 and pf0910.

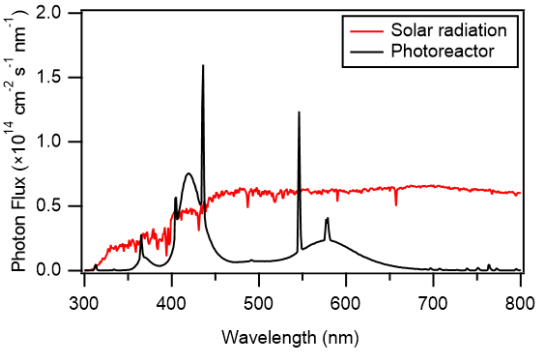

Figure S2. Photon flux inside of the photoreactor (black) and actinic flux for a fall day in Hong Kong in the morning (red). One lamp with output centered at ~365 nm (RPR-3500A, Southern New England Ultraviolet Company), four lamps with outputs centered at ~421 nm (RPR-4190A, Southern New England Ultraviolet Company), and three lamps with outputs centered at ~580 nm (RPR-5750A, Southern New England Ultraviolet Company) were used to illuminate solutions in the photoreactor.

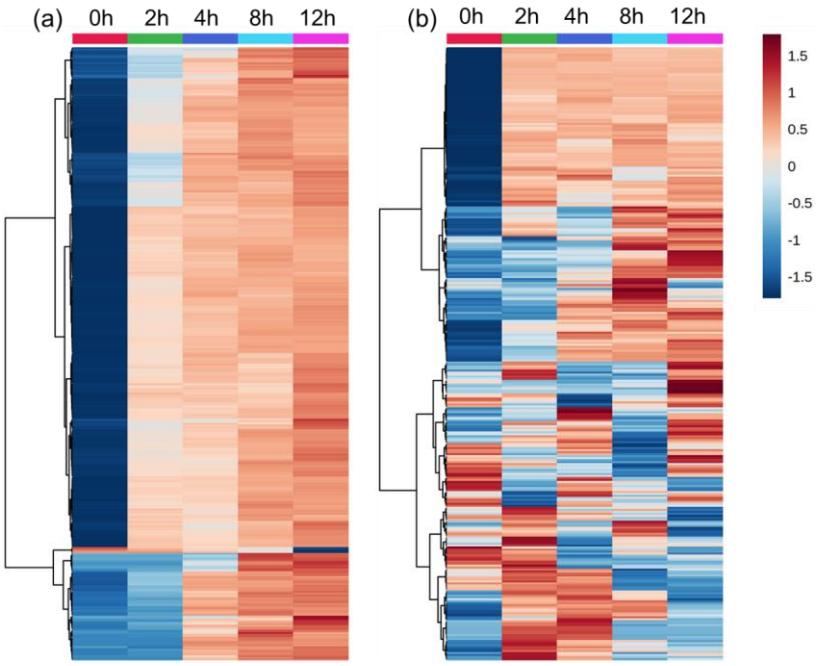

Figure S3. Heat maps showing the time evolution of (a) water-soluble compounds and (b) water-insoluble compounds from *E. hormaechei* B0910 during exposure to simulated sunlight at pH 4.3. The heat maps were generated from non-targeted UPLC-MS analysis of samples with different light exposure times. 259 water-soluble compounds and 215 water-insoluble compounds were selected based on PLS-DA results (VIP > 1.0 criteria). The average UPLC-MS intensity of each compound at each light exposure time was obtained from the nine replicates. The average UPLC-MS intensities were subsequently log10 transformed and auto scaled (i.e., mean-centered and divided by the standard deviation of each variable). The color scale ranges from red color for high abundance to blue for low abundance.

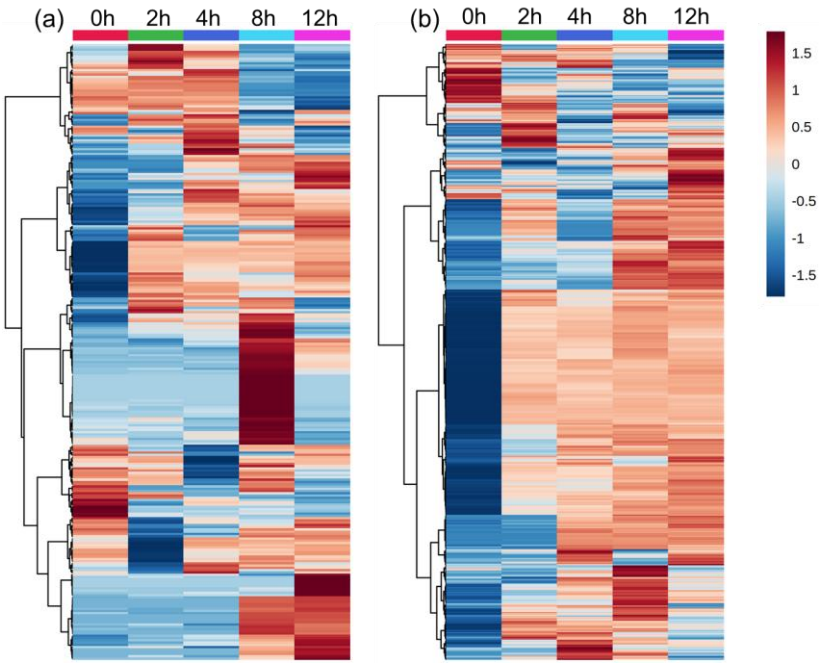

Figure S4. Heat maps showing the time evolution of (a) water-soluble compounds and (b) water-insoluble compounds from *E. hormaechei* pf0910 during exposure to simulated sunlight at pH 4.3. The heat maps were generated from non-targeted UPLC-MS analysis of samples with different light exposure times. 209 water-soluble compounds and 251 water-insoluble compounds were selected based on PLS-DA results (VIP > 1.0 criteria). The average UPLC-MS intensity of each compound at each light exposure time was obtained from the nine replicates. The average UPLC-MS intensities were subsequently log10 transformed and auto scaled (i.e., mean-centered and divided by the standard deviation of each variable). The color scale ranges from red color for high abundance to blue for low abundance.

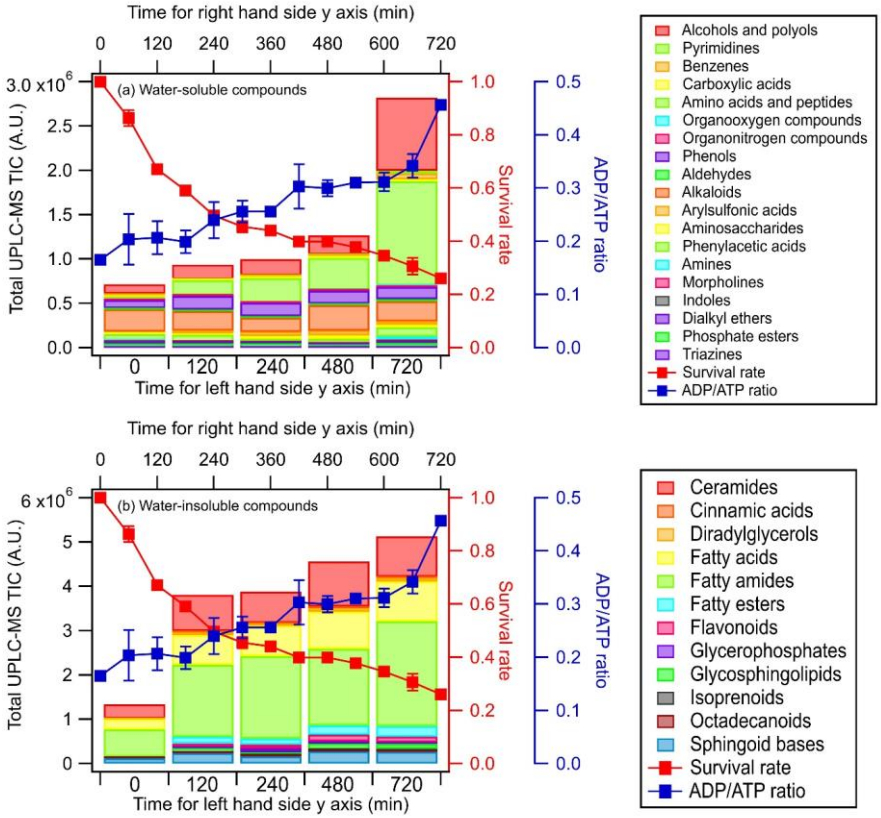

Figure S5. Time evolution of the UPLC-MS total ion chromatograph (TIC) signals of (a) water-soluble compounds, and (b) water-insoluble compounds from *E. hormaechei* pf0910 during exposure to simulated sunlight at pH 4.3 over time. These compounds are classified based on their chemical functionality. Also shown are the time evolution of the survival rate and ADP/ATP ratio of *E. hormaechei* pf0910.

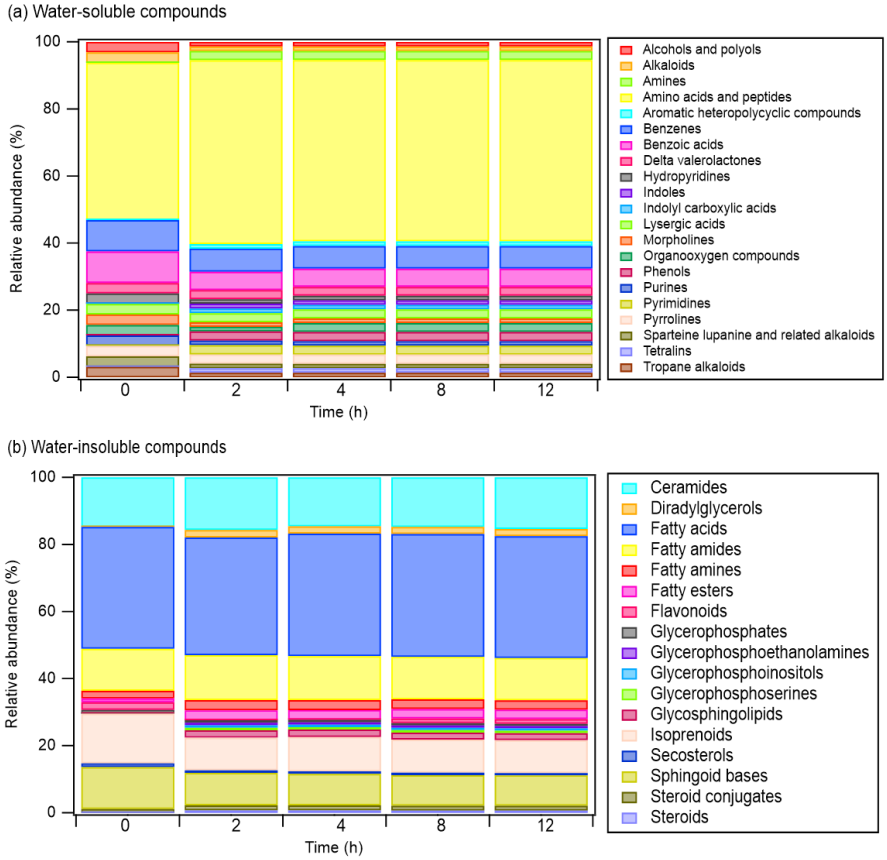

Figure S6. Relative abundance of the different classes of (a) water-soluble compounds, and (b) water-insoluble compounds from *E. hormaechei* B0910 during exposure to simulated sunlight at pH 4.3.

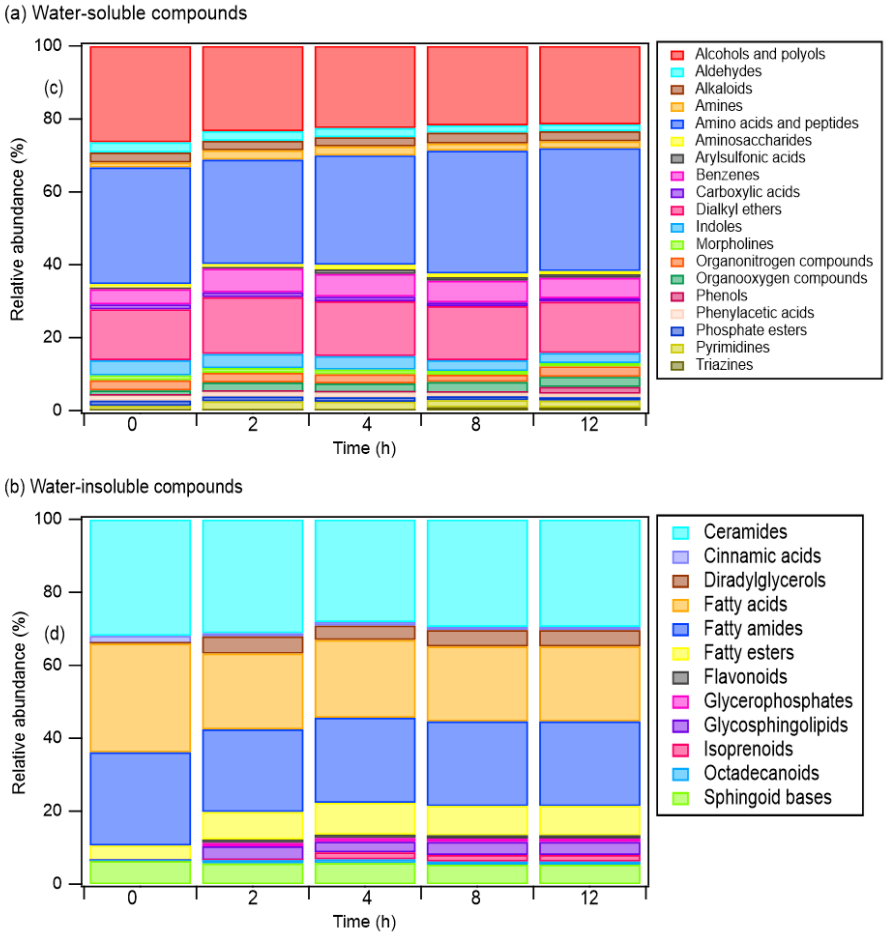

Figure S7. Relative abundance of the different classes of (c) water-soluble compounds, and (d) water-insoluble compounds from *E. hormaechei* pf0910 during exposure to simulated sunlight at pH 4.3.

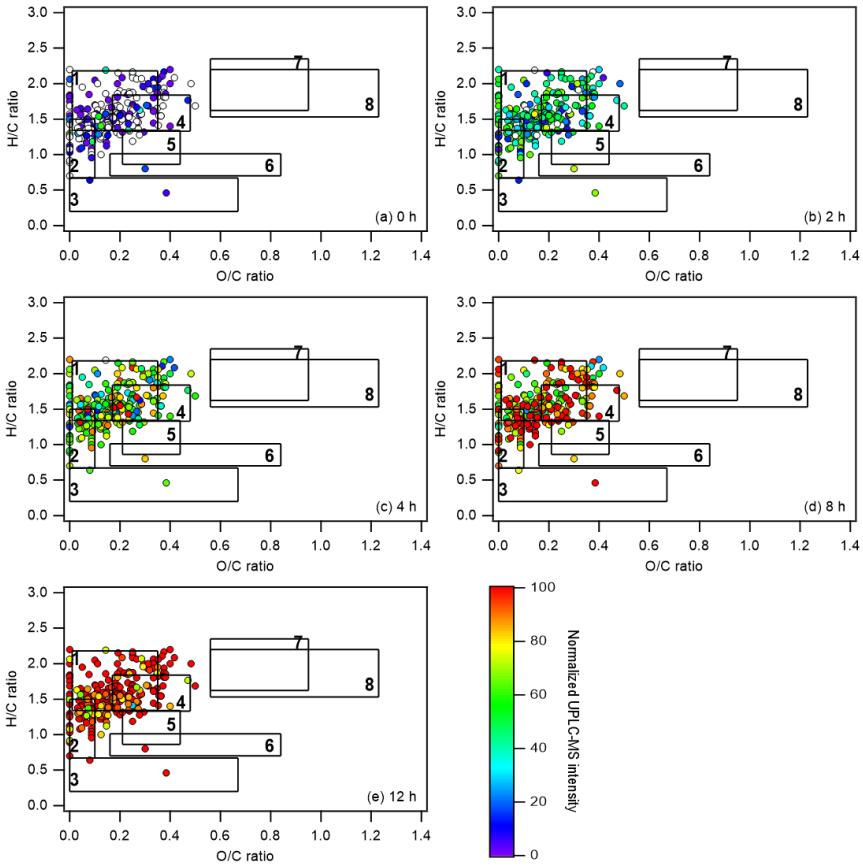

Figure S8. Van Krevelen diagrams of water-soluble compounds from *E. hormaechei* B0910 during exposure to simulated sunlight at pH 4.3 taken at different time points of the experiment: (a) 0 h, (b) 2 h, (c) 4 h, (d) 8 h, and (e) 12 h. The color of each symbol denotes its UPLC-MS intensity at that specific time point normalized to its maximum UPLC-MS intensity obtained during the entire experiment. Symbols that are colored white indicates that these compounds were not detected at that specific time point. The Van Krevelen diagrams are divided into eight chemical classes based on their O/C and H/C ratios: (1) lipids, (2) unsaturated hydrocarbons, (3) condensed aromatic structures, (4) peptides, (5) lignin, (6) tannin, (7) amino sugars, and (8) carbohydrates.

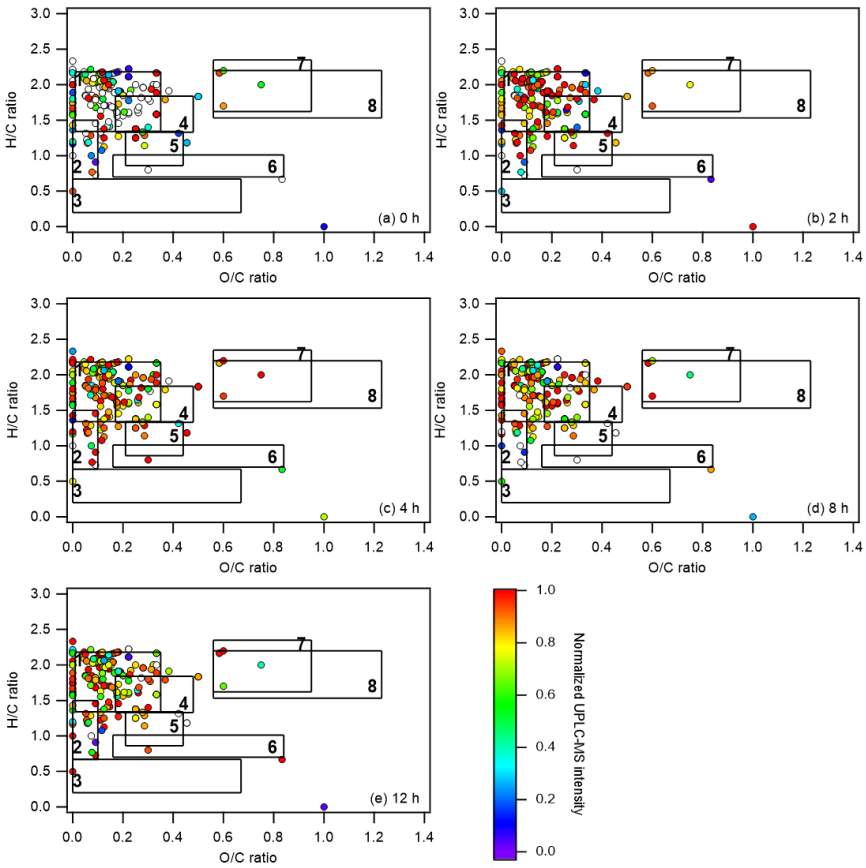

Figure S9. Van Krevelen diagrams of water-insoluble compounds from *E. hormaechei* B0910 during exposure to simulated sunlight at pH 4.3: (a) 0 h, (b) 2 h, (c) 4 h, (d) 8 h, and (e) 12 h. The color of each symbol denotes its UPLC-MS intensity at that specific time point normalized to its maximum UPLC-MS intensity obtained during the entire experiment. Symbols that are colored white indicates that these compounds were not detected at that specific time point. The Van Krevelen diagrams are divided into eight chemical classes based on their O/C and H/C ratios: (1) lipids, (2) unsaturated hydrocarbons, (3) condensed aromatic structures, (4) peptides, (5) lignin, (6) tannin, (7) amino sugars, and (8) carbohydrates.

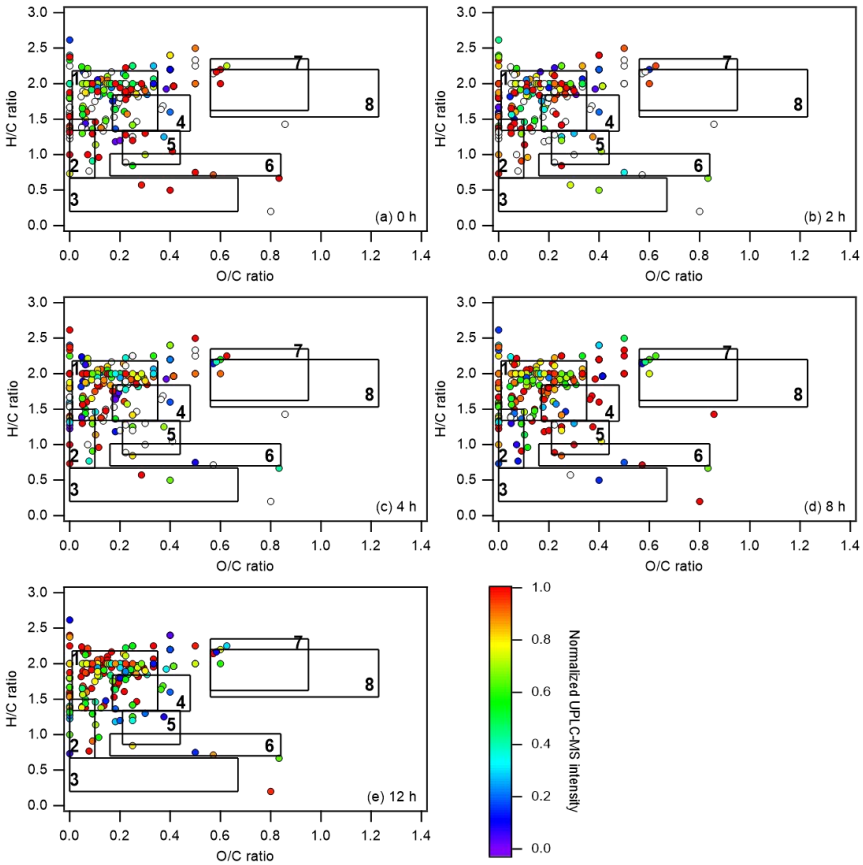

Figure S10. Van Krevelen diagrams of water-soluble compounds from *E. hormaechei* pf0910 during exposure to simulated sunlight at pH 4.3: (a) 0 h, (b) 2 h, (c) 4 h, (d) 8 h, and (e) 12 h. The color of each symbol denotes its UPLC-MS intensity at that specific time point normalized to its maximum UPLC-MS intensity obtained during the entire experiment. Symbols that are colored white indicates that these compounds were not detected at that specific time point. The Van Krevelen diagrams are divided into eight chemical classes based on their O/C and H/C ratios: (1) lipids, (2) unsaturated hydrocarbons, (3) condensed aromatic structures, (4) peptides, (5) lignin, (6) tannin, (7) amino sugars, and (8) carbohydrates.

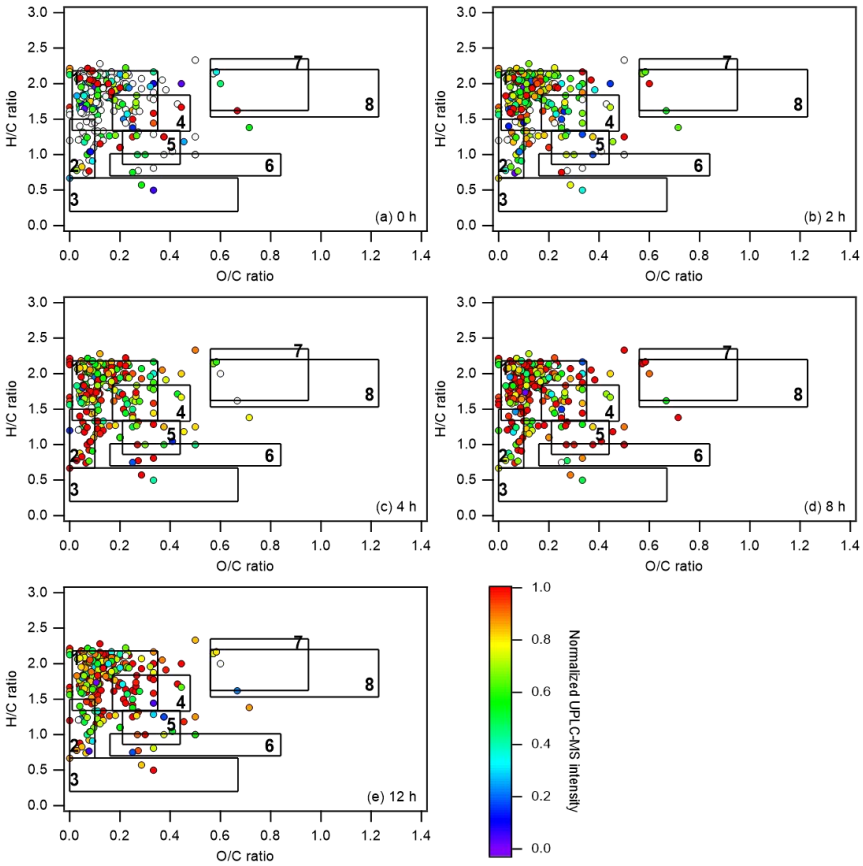

Figure S11. Van Krevelen diagrams of water-insoluble compounds from *E. hormaechei* pf0910 during exposure to simulated sunlight at pH 4.3: (a) 0 h, (b) 2 h, (c) 4 h, (d) 8 h, and (e) 12 h. The color of each symbol denotes its UPLC-MS intensity at that specific time point normalized to its maximum UPLC-MS intensity obtained during the entire experiment. Symbols that are colored white indicates that these compounds were not detected at that specific time point. The Van Krevelen diagrams are divided into eight chemical classes based on their O/C and H/C ratios: (1) lipids, (2) unsaturated hydrocarbons, (3) condensed aromatic structures, (4) peptides, (5) lignin, (6) tannin, (7) amino sugars, and (8) carbohydrates.

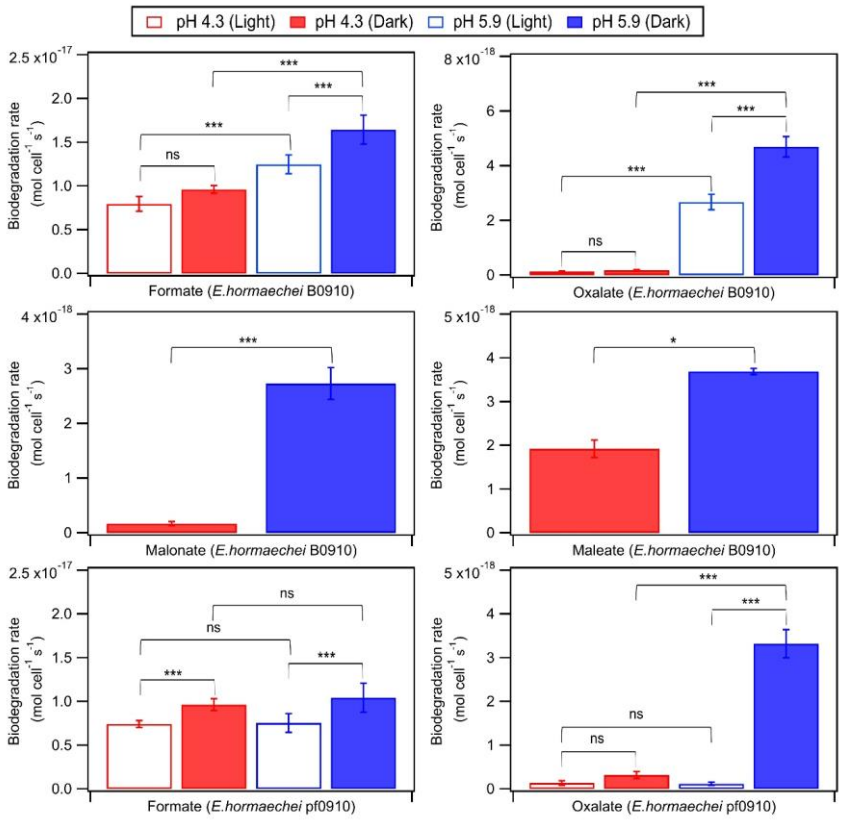

105

106 **Figure S12.** Biodegradation rates of oxalate, maleate, and malonate by (a) *E. hormaechei*
107 B0910 and (b) *E. hormaechei* pf0910 under light and dark conditions at pH 4.3 and pH 5.9.
108 Error bars represent one standard deviation from the mean of biological triplicates. Statistical
109 analysis was performed using the Student's t test (ns: not significant, *: p value < 0.05, **: p
110 value < 0.01, ***: p value < 0.001).

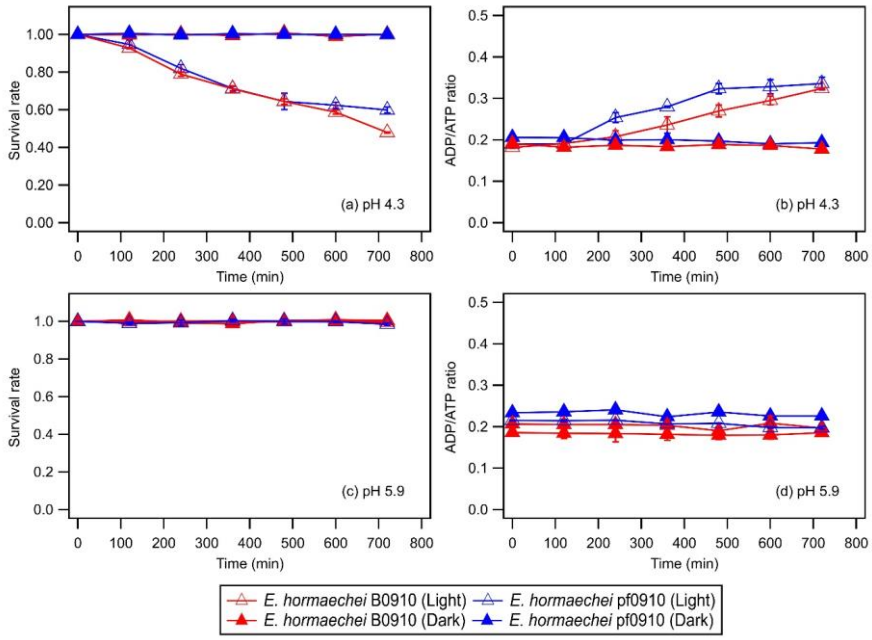

Figure S13. Survival and ADP/ATP ratios of *E. hormaechei* B0910 and *E. hormaechei* pf0910 under illuminated and dark conditions at pH 4.3 and pH 5.9 in the solutions containing the seven organic acids. Error bars represent one standard deviation from the mean of biological triplicates.

Deleted: carboxylic

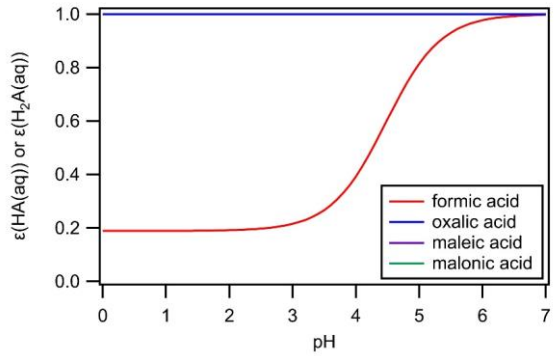

Figure S14. Calculated pH-dependent molar fraction of formic acid in the aqueous phase ($\varepsilon(HA(aq))$) and pH-dependent molar fractions of oxalic acid, malonic acid, and maleic acid in the aqueous phase ($\varepsilon(H_2A(aq))$) under cloud water conditions (Section S6 and Table S8). A liquid water concentration of 10^6 μg m^{-3} (Ervens et al., 2011) was assumed in these calculations. A significant fraction of formic acid will be in the gas phase at pH 4 and 5 under cloud water conditions, whereas all of the oxalic acid, malonic acid, and maleic acid will be in the aqueous phase at pH 4 and 5 under cloud water conditions (note that their values overlap one another at $\varepsilon(H_2A(aq)) = 1$). These differences were due primarily to the large differences in their water solubility (i.e., Henry's law constants) (Table S8).

Formatted: Centered

Formatted: Superscript

Formatted: Font: Not Bold

Table S1. Chemical composition of the artificial cloud water used to prepare bacterial cells and perform experiments that investigated the effects of cloud water pH and light exposure on the survival and energetic metabolism of bacteria. In the experiments, the pH of the artificial cloud water was adjusted while keeping the final organic and inorganic ion composition the same.

Organic ion	μM	Inorganic ion	μM
Formate	17.1	Na^+	93
Acetate	10.2	NH_4^+	235
Pyruvate	2.7	K^+	8
Oxalate	10.3	Mg^{2+}	23
		Ca^{2+}	49
		Cl^-	138
		SO_4^{2-}	305

Table S2. Chemical composition of the artificial cloud water used for organic acid biodegradation experiments.

Organic ion	μM	Inorganic ion	μM
Formate	50	Na^+	930
Acetate	50	NH_4^+	2350
Pyruvate	50	K^+	80
Oxalate	50	Mg^{2+}	230
Succinate	50	Ca^{2+}	490
Maleate	50	Cl^-	1380
Malonate	50	SO_4^{2-}	3050
Glutarate	50		
MSA	50		

Deleted: carboxylic

Table S3. Genes involved in the pH homeostasis in the two *E. hormaechei* strains.

Transporters	Protein subunits	*E. hormaechei B0910*	*E. hormaechei pf0910*
		CDS	CDS
F1F0-type ATP synthase	Subunit a, AtpB	MOG78_16595	MMW20_13045
	Subunit c, AtpE	MOG78_16590	MMW20_13050
	Subunit b, AtpF	MOG78_16585	MMW20_13055
	Subunit delta, AtpH	MOG78_16580	MMW20_13060
	Subunit alpha, AtpA	MOG78_16575	MMW20_13065
	Subunit gamma, AtpG	MOG78_16570	MMW20_13070
	Subunit beta, AtpD	MOG78_16565	MMW20_13075
	Subunit epsilon, AtpC	MOG78_16560	MMW20_13080
Kdp-type high-affinity potassium transporter	Potassium-binding ATPase subunit KdpA	MOG78_10080	MMW20_19865
	Potassium-binding ATPase subunit KdpB	MOG78_10085	MMW20_19860
	Potassium-binding ATPase subunit KdpC	MOG78_10090	MMW20_19855
	Potassium-binding ATPase subunit KdpF	MOG78_10075	Gene sequence found but CDS is not annotated. (Chromosome genome nucleotide position: 3800683-3800772)
Kup-type low-affinity potassium transporter	Kup	MOG78_16640	MMW20_13000

Formatted: Font: 12 pt

Table S4. Stoichiometric ranges of the eight chemical classes in VK diagrams (Bauer et al., 2002; Jaenicke, 2005).

Chemical class	H/C	O/C
Amino sugar (Burrows et al., 2009)	$1.62 \leq H/C \leq 2.35$	$0.56 \leq O/C \leq 0.95$
Carbohydrate (Jaenicke, 2005)	$1.53 \leq H/C \leq 2.20$	$0.56 \leq O/C \leq 1.23$
Lignin (Möhler et al., 2007)	$0.86 \leq H/C \leq 1.34$	$0.21 \leq O/C \leq 0.44$
Lipid (Burrows et al., 2009)	$1.34 \leq H/C \leq 2.18$	$0.01 \leq O/C \leq 0.35$
Peptide (Attard et al., 2012)	$1.33 \leq H/C \leq 1.84$	$0.17 \leq O/C \leq 0.48$
Tannin (Hu et al., 2018)	$0.70 \leq H/C \leq 1.01$	$0.16 \leq O/C \leq 0.84$
Unsaturated hydrocarbons (Amato et al., 2005)	$0.67 \leq H/C \leq 1.5$	$0 \leq O/C \leq 0.10$
Condensed aromatic structures (Delort et al., 2010)	$0.20 \leq H/C \leq 0.67$	$0 \leq O/C \leq 0.67$

Deleted: S3

Table S5. Genes involved in the biodegradation of organic acids in the two *E. hormaechei* strains.

Organic acid	Genes	*E. hormaechei B0910*		*E. hormaechei pf0910*	
		Biodegradation	CDS	Biodegradation	CDS
		Yes/No	Absent/Present	Yes/No	Absent/Present
Formic acid	Formate dehydrogenase	Yes	MOG78_16880; MOG78_16875; MOG78_16870; MOG78_06810	Yes	MMW20_12765; MMW20_12770; MMW20_12775; MMW20_22665
Oxalic acid	Oxalate decarboxylase	Yes	Absent	Yes	Absent
	Oxalate oxidase	Yes	Absent	Yes	Absent
	Formyl-CoA:oxalate CoA-transferase	Yes	Absent	Yes	Absent
	Succinyl-CoA:oxalate CoA-transferase	Yes	Absent	Yes	Absent
	Hypothetical protein (Cupin 2 protein)[a]	Yes	MOG78_20825	Yes	MMW20_08875
Malonic acid	Malonate decarboxylase	Yes	MOG78_18565; MOG78_18550; MOG78_18545; MOG78_18540; MOG78_18530	No	MMW20_11060; MMW20_11075; MMW20_11080; MMW20_11085; MMW20_11095
	Malonate CoA-transferase	Yes	Absent	No	Absent
	Malonate-semialdehyde dehydrogenase	Yes	Absent	No	Absent
	Malonyl-CoA/methylmalonyl-CoA synthetase	Yes	Absent	No	Absent
Maleic acid	Maleate isomerase	Yes	Absent	No	Absent
	Maleate hydratase	Yes	Absent	No	Absent
	3-isopropylmalate dehydratase[a]	Yes	MOG78_13080; MOG78_13075	No	MMW20_17000; MMW20_17005
Acetic acid	Acetyl-CoA synthetase	No	MOG78_14765	No	MMW20_14980
	Acetate kinase	No	MOG78_01250	No	MMW20_05785
	Aldehyde dehydrogenase	No	MOG78_17415	No	MMW20_12230
	ActP[b]	No	MOG78_14775	No	MMW20_14970

Deleted: S4
Deleted: carboxylic
Deleted: Carboxylic
Formatted Table

	SatP[b]	No	MOG78_13285	No	MMW20_16750
Methane sulfonic acid	Alkanesulfonate monooxygenase	No	MOG78_08820; MOG78_08810	No	MMW20_21175; MMW20_21185
Glutaric acid	Succinate-semialdehyde dehydrogenase / glutarate-semialdehyde dehydrogenase[c]	No	MOG78_19060; MOG78_13695	No	MMW20_10560; MMW20_16345
	Glutaryl-CoA synthetase	No	Absent	No	Absent
	Glutarate dioxygenase	No	Absent	No	Absent

[a] Genes are not canonical but may involve in the biodegradation of organic acids.

[b] Transporter proteins involved in uptake of acetic acid for biodegradation

[c] No reverse catalysis in the direction from glutarate to glutarate-semialdehyde has been reported in the literature.

Table S6. Concentration of radicals and cells used to estimate the loss rates by biodegradation and chemical reactions in Table S6.

Radical concentration/ Cell concentration	Area	Concentration	Reference
·OH (M)	Remote	2.2×10^{-14}	(Vaitilingom et al., 2010)
	Marine	2.0×10^{-12}	(Vaitilingom et al., 2013)
	Urban	3.5×10^{-15}	(Morris et al., 2014)
NO_3· (M)	Remote	5.1×10^{-15}	(Morris et al., 2017)
	Marine	6.9×10^{-15}	(Hu et al., 2018)
	Urban	1.4×10^{-13}	(Huang et al., 2021)
Cell (cell L^{-1})		8.0×10^{7}	(Zhang et al., 2021)

Table S7. Estimations of the loss rates of formate, oxalate, and malonate by biodegradation and chemical reactions (i.e., ·OH oxidation (daytime) and NO_3· (nighttime)). These loss rates were calculated based on concentrations and pH measured at the different sites. Equations used in these calculations can be found in Section S6. References used to obtain the pH of cloud/rainwater and organic acids are indicated in superscripts. The biodegradation and chemical reaction loss rates calculated here were used to generate Figure 5.

Daytime

Location (remote)	Category	pH	Formate (μM)	Formate loss rate (M s^{-1})			Oxalate (μM)	Oxalate loss rate (M s^{-1})		
				bio (pH ~4)	bio (pH ~5)	·OH (remote)		bio (pH ~4)	bio (pH ~5)	·OH (remote)
Mount Lu(Möhler et al., 2007)	Cloud	3.81 (Vaïtilingom et al., 2012)	10.83 (Wei et al., 2017)	1.34×10^{-10}		5.72×10^{-10}	4.95 (Zhu et al., 2018)	1.06×10^{-12}		1.74×10^{-11}
Mount Lu(Wei et al., 2017)	Rain	4.44 (Peng et al., 2019)	10.21 (Amato et al., 2005)	1.26×10^{-10}		5.39×10^{-10}	2.54 (Burrows et al., 2009)	5.44×10^{-13}		8.92×10^{-12}
Mount Heng(Amato et al., 2017)	Cloud	3.8 (Amato et al., 2005)	19.65 (Amato et al., 2017)	2.43×10^{-10}		1.04×10^{-9}	5.11 (Wei et al., 2017)	1.10×10^{-12}		1.80×10^{-11}
Mount Heng(Delort et al., 2010)	Rain	4.35 (Vaitilingom et al., 2010)	14.30 (Vaitilingom et al., 2013)	1.77×10^{-10}		7.55×10^{-10}	1.66 (Ervens and Amato, 2020)	3.55×10^{-13}		5.83×10^{-12}
Mangdang Mountain(Ariya et al., 2002)	Rain	4.81 (Husárová et al., 2011)	7.90 (Vaïtilingom et al., 2011)	9.78×10^{-11}		4.17×10^{-10}	1.80 (Jaber et al., 2020)	3.86×10^{-13}		6.34×10^{-12}
Taiwan(Jaber et al., 2021)	Cloud	3.91 (Joly et al., 2015)	5.74 (Davey and O'toole, 2000)	7.11×10^{-11}		3.03×10^{-10}	6.60 (Delort et al., 2010)	1.42×10^{-12}		2.32×10^{-11}
Kleiner Feldberg, Germany(Flemming and Wingender, 2010)	Cloud	3.9-4.6 (Vaïtilingom et al., 2012)	3.26 (Matulova et al., 2014)	4.03×10^{-11}		1.72×10^{-10}	ND			
Whiteface Mountain, USA(Amato et al., 2005)	Cloud	3.1-4.4 (Peng et al., 2019)	25.20 (Amato et al., 2005)	3.12×10^{-10}		1.33×10^{-9}	9.66 (Pye et al., 2020)	2.07×10^{-12}		3.40×10^{-11}
Rax, Austria(Shah et al., 2020)	Cloud	3.84 (Li et al., 2020)	13.25 (Pye et al., 2020)	1.64×10^{-10}		7.00×10^{-10}	5.11 (Shah et al., 2020)	1.10×10^{-12}		1.80×10^{-11}
Sonnblick, Austria(Qu and Han, 2021)	Cloud	5.0-6.5 (Anglada et al., 2015)	6.30 (Joly et al., 2015)		9.79×10^{-11}	3.33×10^{-10}	1.89 (Vaïtilingom et al., 2011)		3.61×10^{-12}	6.65×10^{-12}
Mount Tai, China(Joly et al., 2015)	Cloud	4.6 (Jaber et al., 2021)	31.80 (Jaber et al., 2020)	3.94×10^{-10}		1.68×10^{-9}	11.10 (Li et al., 2020)	2.38×10^{-12}		3.91×10^{-11}
Shangzhong(Qu and Han, 2021)	Rain	ND	4.95 (Peng et al., 2019)	6.13×10^{-11}		2.61×10^{-10}	1.16 (Chen et al., 2012)	2.48×10^{-13}		4.07×10^{-12}
São Paulo State, Brazil(Després et al., 2012)	Rain	4.96 (Ding et al., 2015)	7.80 (Zhou et al., 2018)		1.21×10^{-10}	4.12×10^{-10}	1.20 (Prokof'eva et al., 2021)		2.29×10^{-12}	4.22×10^{-12}

Location (Marine)	Category	pH	Formate (μM)	Formate loss rate (M s^{-1})			Oxalate (μM)	Oxalate loss rate (M s^{-1})		
				bio (pH ~4)	bio (pH ~5)	·OH (marine)		bio (pH ~4)	bio (pH ~5)	·OH (marine)
Puerto Rico	Cloud	5.5 (Romano et al., 2019)	1.00 (Ruiz-Gil et al., 2020)		1.55×10^{-11}	4.80×10^{-9}	0.50 (Romano et al., 2021)		9.55×10^{-13}	1.60×10^{-10}
Puerto Rico(Tsai and Kuo, 2013)	Rain	5.3 (Löflund et al., 2002)	0.20 (Sun et al., 2016)		3.11×10^{-12}	9.60×10^{-10}	0.00 (Li et al., 2020)			

Deleted: S6

Deleted: carboxylic

Puy de dome(Vaitilingom et al., 2010)	Cloud	6.1 (Vaïtilingom et al., 2011)	4.90 (George et al., 2015)		7.61×10^{-11}	2.35×10^{-8}	1.00 (Huang et al., 2018)		1.91×10^{-12}	3.20×10^{-10}

Location (Urban)			Formate (μM)	Formate loss rate (M s^{-1})			Oxalate (μM)	Oxalate loss rate (M s^{-1})		
				bio (pH ~4)	bio (pH ~5)	·OH (urban)		bio (pH ~4)	bio (pH ~5)	·OH (urban)
Shenzhen, South China(Misovich et al., 2021)	Rain	4.56 (Li et al., 2020)	2.26 (Tsai and Kuo, 2013)	2.80×10^{-11}		1.90×10^{-11}	0.58 (Löflund et al., 2002)	1.23×10^{-13}		3.22×10^{-13}
Anshun(Sun et al., 2016)	Rain	4.67 (Li et al., 2020)	8.77 (Vaitilingom et al., 2010)	1.09×10^{-10}		7.37×10^{-11}	2.84 (Jaber et al., 2020)	6.09×10^{-13}		1.59×10^{-12}
Newark US East Coast(Jaber et al., 2021)	Rain	4.6 (Vaïtilingom et al., 2011)	4.44 (Jaber et al., 2020)	5.50×10^{-11}		3.73×10^{-11}	0.68 (Jaber et al., 2021)	1.46×10^{-13}		3.81×10^{-13}
Hong Kong SAR(Bearson et al., 1997)	Cloud	3.87 (Lund et al., 2014)	17.10 (Bearson et al., 1997)	2.12×10^{-10}		1.44×10^{-10}	10.30 (Davey and O'toole, 2000)	2.21×10^{-12}		5.77×10^{-12}
Puy de dome(Delort et al., 2010)	Cloud	3.9 (Flemming and Wingender, 2010)	33.20 (Vaïtilingom et al., 2012)	4.11×10^{-10}		2.79×10^{-10}	9.30 (Matulova et al., 2014)	1.99×10^{-12}		5.21×10^{-12}

ND: No data

Nighttime

Location (remote)	Category	pH	Formate (μM)	Formate loss rate (M s^{-1})			Oxalate (μM)	Oxalate loss rate (M s^{-1})			Malonate (μM)	Malonate loss rate (M s^{-1})		
				bio (pH ~4)	bio (pH ~5)	NO_3· (remote)		bio (pH ~4)	bio (pH ~5)	NO_3· (remote)		bio (pH ~4)	bio (pH ~5)	NO_3· (remote)
Mount Lu(Guan and Liu, 2020)	Cloud	3.81 (Davey and O'toole, 2000)	10.83 (Delort et al., 2010)	1.69×10^{-10}		2.32×10^{-12}	4.95 (Flemming and Wingender, 2010)	2.07×10^{-12}		1.11×10^{-12}	ND			
Mount Lu(Vaïtilingom et al., 2012)	Rain	4.44 (Matulova et al., 2014)	10.21 (Bianco et al., 2018)	1.59×10^{-10}		2.19×10^{-12}	2.54 (Laszakovits and Mackay, 2022)	1.06×10^{-12}		5.69×10^{-13}	ND			
Mount Heng(Watson et al., 2007)	Cloud	3.8 (Rivas-Ubach et al., 2018)	19.65 (Matulova et al., 2014)	3.06×10^{-10}		4.21×10^{-12}	5.11 (Bianco et al., 2016)	2.14×10^{-12}		1.15×10^{-12}	ND			
Mount Heng(Tyagi et al., 2015)	Rain	4.35 (Jaber et al., 2021)	14.30 (Bianco et al., 2019)	2.23×10^{-10}		3.06×10^{-12}	1.66 (Vaitilingom et al., 2010)	6.94×10^{-13}		3.71×10^{-13}	ND			
Mangdang Mountain(Vaïtilingom et al., 2011)	Rain	4.81 (Fankhauser et al., 2019)	7.90 (Makuc et al., 2001)	1.23×10^{-10}		1.69×10^{-12}	1.80 (Tilgner et al., 2021)	7.55×10^{-13}		4.04×10^{-13}	1.40 (Koutny et al., 2006)		5.16×10^{-12}	4.00×10^{-14}
Taiwan(Guan and Liu, 2020)	Cloud	3.91 (Vaïtilingom et al., 2011)	5.74 (Jaber et al., 2020)	8.95×10^{-11}		1.23×10^{-12}	6.60 (Jaber et al., 2021)	2.77×10^{-12}		1.48×10^{-12}	0.16 (Herrmann et al., 2010)	3.65×10^{-14}		4.57×10^{-15}

Kleiner Feldberg, Germany(Vaïtilingom et al., 2011)	Cloud	3.9-4.6 (Jaber et al., 2020)	3.26 (Jaber et al., 2021)	5.08×10^{-11}		6.98×10^{-13}	ND				ND				
Whiteface Mountain, USA(Herrmann et al., 2010)	Cloud	3.1-4.4 (Ervens et al., 2003)	25.20 (Herrmann et al., 2010)	3.93×10^{-10}		5.40×10^{-12}	9.66 (Vaitilingom et al., 2010)	4.05×10^{-12}		2.17×10^{-12}	7.69 (Vaïtilingom et al., 2011)	1.75×10^{-12}		2.20×10^{-13}
Rax, Austria(Fankhauser et al., 2019)	Cloud	3.84 (Pye et al., 2020)	13.25 (Li et al., 2020)	2.07×10^{-10}		2.84×10^{-12}	5.11 (Pye et al., 2020)	2.14×10^{-12}		1.15×10^{-12}	1.92 (Shah et al., 2020)	4.38×10^{-13}		5.49×10^{-14}
Sonnblick, Austria(Qu and Han, 2021)	Cloud	5.0-6.5 (Vaïtilingom et al., 2012)	6.30 (Zhu et al., 2018)		1.32×10^{-10}	1.35×10^{-12}	1.89 (Peng et al., 2019)		1.19×10^{-11}	4.24×10^{-13}	0.38 (Ariya et al., 2002)		1.42×10^{-12}	1.10×10^{-14}
Mount Tai, China(Vaitilingom et al., 2010)	Cloud	4.6 (Husárová et al., 2011)	31.80	4.96×10^{-10}		6.81×10^{-12}	11.10 (Vaïtilingom et al., 2011)	4.65×10^{-12}		2.49×10^{-12}	ND			
Shangzhong(Xu et al., 2009)	Rain		4.95	7.71×10^{-11}		1.06×10^{-12}	1.16	4.84×10^{-13}		2.59×10^{-13}	ND			
São Paulo State, Brazil(Coelho et al., 2011)	Rain	4.96 (Coelho et al., 2011)	7.80 (Coelho et al., 2011)		1.63×10^{-10}	1.67×10^{-12}	1.20 (Coelho et al., 2011)		7.57×10^{-12}	2.69×10^{-13}	ND			

				Formate loss rate ($M\ s^{-1}$)				Oxalate loss rate ($M\ s^{-1}$)				Malonate loss rate ($M\ s^{-1}$)		
Location (marine)		pH	Formate (μM)	bio (pH ~4)	bio (pH ~5)	$NO_3\cdot$ (marine)	Oxalate (μM)	bio (pH ~4)	bio (pH ~5)	$NO_3\cdot$ (marine)	Malonate (μM)	bio (pH ~4)	bio (pH ~5)	$NO_3\cdot$ (marine)
Puerto Rico(Gioda et al., 2011)	Cloud	5.5 (Gioda et al., 2011)	1.00 (Gioda et al., 2011)		2.09×10^{-11}	2.90×10^{-13}	0.50 (Gioda et al., 2011)		3.16×10^{-12}	1.52×10^{-13}	ND			
	Rain	5.3 (Gioda et al., 2011)	0.20 (Gioda et al., 2011)		4.19×10^{-12}	5.80×10^{-14}	ND				ND			
Puy de dôme(Vaitilingom et al., 2013)	Cloud	6.1 (Vaitilingom et al., 2013)	4.90 (Vaitilingom et al., 2013)		1.03×10^{-10}	1.42×10^{-12}	1.00 (Vaitilingom et al., 2013)		6.31×10^{-12}	3.04×10^{-13}	0.40 (Vaïtilingom et al., 2012)		1.47×10^{-12}	1.55×10^{-14}

				Formate loss rate ($M\ s^{-1}$)				Oxalate loss rate ($M\ s^{-1}$)				Malonate loss rate ($M\ s^{-1}$)		
Location (urban)		pH	Formate (μM)	bio (pH ~4)	bio (pH ~5)	$NO_3\cdot$ (urban)	Oxalate (μM)	bio (pH ~4)	bio (pH ~5)	$NO_3\cdot$ (urban)	Malonate (μM)	bio (pH ~4)	bio (pH ~5)	$NO_3\cdot$ (urban)
Shenzhen, South China(Huang et al., 2010)	Rain	4.56 (Huang et al., 2010)	2.26 (Huang et al., 2010)	3.52×10^{-11}		1.33×10^{-11}	0.58 (Huang et al., 2010)	2.41×10^{-13}		3.54×10^{-12}	ND			
Anshun(Zhang et al., 2011)	Rain	4.67 (Zhang et al., 2011)	8.77 (Zhang et al., 2011)	1.37×10^{-10}		5.16×10^{-11}	2.84 (Zhang et al., 2011)	1.19×10^{-12}		1.75×10^{-11}	ND			
Newark US East Coast(Song and Gao, 2009)	Rain	4.6 (Song and Gao, 2009)	4.44 (Song and Gao, 2009)	6.92×10^{-11}		2.61×10^{-11}	0.68 (Song and Gao, 2009)	2.85×10^{-13}		4.19×10^{-12}	0.29(Song and Gao, 2009)	6.61×10^{-14}		2.27×10^{-13}
Hong Kong SAR(Li et al., 2020)	Cloud	3.87 (Li et al., 2020)	17.10 (Li et al., 2020)	2.66×10^{-10}		1.01×10^{-10}	10.30 (Li et al., 2020)	4.32×10^{-12}		6.34×10^{-11}	1.36 (Zhao et al., 2019)	3.10×10^{-13}		1.07×10^{-12}
Puy de dome(Vaitilingom et al., 2013)	Cloud	3.9 (Vaitilingom et al., 2013)	33.20 (Vaitilingom et al., 2013)	5.17×10^{-10}		1.95×10^{-10}	9.30 (Vaitilingom et al., 2013)	3.90×10^{-12}		5.73×10^{-11}	3.50 (Vaitilingom et al., 2013)	7.97×10^{-13}		2.74×10^{-12}

197 ND: No data

Table S8. Acid dissociation constants and Henry's law coefficients at 25 °C used to generate $\varepsilon(HA(aq))$ and $\varepsilon(H_2A(aq))$ S curves in Figure S14

Organic acid	First acid dissociation constant (K_{a1}) (mol L^{-1})	Second acid dissociation constant (K_{a2}) (mol L^{-1})	Henry's law constant (H_{HA} or H_{H_2A}) (mol L^{-1} atm^{-1})
Formic acid	1.78×10^{-4} (Haynes, 2014)	Not applicable	9.53×10^{3}
Oxalic acid	5.62×10^{-2} (Haynes, 2014)	1.55×10^{-4} (Haynes, 2014)	6.11×10^{8} (Nah et al., 2018)[a]
Malonic acid	1.48×10^{-3} (Williams, 2022)	2.04×10^{-6} (Williams, 2022)	3.85×10^{10} (Compernolle and Müller, 2014)
Maleic acid	1.26×10^{-2} (Weast and Astle, 1981)	8.51×10^{-7} (Weast and Astle, 1981)	1.42×10^{10} (Lide and Frederikse, 1995)

[a]While we used the Henry's law coefficient provided by Nah et al. (2018), it should be noted that the authors obtained this value by taking the average of $H_{C_2H_2O_4}$ values provided by Clegg et al. (1996), Compernolle and Muller (2014), and Saxena and Hildemann (1996), and accounted for the effect of temperature using the equations provided by Sander (2015).

Section S1. Genome assembly, annotation, and taxonomic analysis

Genome assembly of the sequencing reads was performed using the NECAT pipeline (v0.0.1_update20200803) (Chen et al., 2021) with the default parameters. The reads were first corrected (PREP_OUTPUT_COVERAGE = 40, CNS_OUTPUT_COVERAGE = 30, MIN_READ_LENGTH = 3000) and then the corrected reads were assembled (OVLP_FAST_OPTIONS = -n 500 -z 20 -b 2000 -e 0.5 -j 0 -u 1 -a 1000, OVLP_SENSITIVE_OPTIONS = -n 500 -z 10 -e 0.5 -j 0 -u 1 -a 1000). Both the correction and assembly steps were progressive with multiple processing steps to improve the accuracy and completeness. The quality of the assembled genomes was evaluated using the Benchmarking Universal Single-copy Orthologs (BUSCO v5.3.1) tool based on the database of enterobacterales_odb10 (Manni et al., 2021). For both strains B00910 and pf0910, complete circular chromosomes and plasmids were obtained.

Genome annotation was performed using Prokka (v1.14.6) (Seemann, 2014) with the default parameters. Whole genome-based taxonomic analysis was conducted using the Type

Formatted: Font: 12 pt
Formatted: Font: 12 pt
Formatted: Font: 12 pt
Formatted ...
Formatted Table
Formatted: Superscript
Formatted: Superscript
Formatted ...
Formatted: Space After: 0 pt, Line spacing: single
Formatted: Space After: 0 pt, Line spacing: single
Formatted: Space After: 0 pt, Line spacing: single
Formatted: Superscript
Formatted: Space After: 0 pt, Line spacing: single
Formatted: Space After: 0 pt, Line spacing: single
Formatted: Space After: 0 pt, Line spacing: single
Formatted: Space After: 0 pt, Line spacing: single
Formatted: Space After: 0 pt, Line spacing: single
Formatted: Space After: 0 pt, Line spacing: single
Formatted: Space After: 0 pt, Line spacing: single
Formatted: Space After: 0 pt, Line spacing: single
Formatted: Superscript
Formatted: Line spacing: single
Formatted: Font: 12 pt
Formatted: Font: 12 pt
Formatted: Font: 12 pt
Formatted: Font: 12 pt
Formatted: Font: 12 pt
Formatted: Font: 12 pt
Formatted: Font: 12 pt
Formatted: Font: 12 pt
Formatted: Font: 12 pt
Deleted: (Zhu et al., 2018)
Formatted: Font: 12 pt
Formatted: Font: 12 pt
Formatted: Font: 12 pt
Formatted: Font: 12 pt
Formatted: Font: 12 pt
Formatted: Font: 12 pt
Formatted: Font: Not Bold

(Strain) Genome Server (TYGS) (Meier-Kolthoff and Göker, 2019). Average Nucleotide Identity (ANI) was calculated by fastANI (v1.33) (Jain et al., 2018). Metabolic pathways were analyzed using the KEGG Mapper (Kanehisa et al., 2022) and the RAST server (Aziz et al., 2008). The sequences of the two genomes have been deposited in NCBI under the BioProject number PRJNA812965.

Section S2. Extraction of water-insoluble and water-soluble biological material and organic compounds for UPLC-MS analysis

A modified Bligh & Dyer (BD) protocol was performed to extract water-insoluble organic compounds (Sündermann et al., 2016). Briefly, 3 mL of methanol (Duskan, LC-MS grade)/chloroform (RCI, HPLC grade) (1:2, v/v) was added to a filtered 5 mL sample solution and vortexed for 5 min, after which the samples were centrifuged at 3000 rpm for 10 min at 10 ℃. The bottom layer was collected into a clean 2 mL centrifuge tube and dried in a concentrator using nitrogen gas. The dried extracts were redissolved in 500 µL of acetonitrile (Duskan, LC-MS grade) and stored at -20 ℃ prior to UPLC-MS analysis. Solid-phase extraction (SPE) was performed to remove the inorganic salts and extract the water-soluble organic compounds using hydrophobic lipophilic balanced (HLB) cartridges (Oasis HLB, 6cc 500 mg). The HLB cartridges were first preconditioned with 1 mL methanol and 2 mL Milli-Q water. A 10 mL filtered sample solution was then loaded into the SPE cartridge and washed with 20 mL Milli-Q water under vacuum at a flow rate of 5 mL/min. The elution was performed by adding 1.5 mL methanol (Duskan, LC-MS grade). The eluent was evaporated to dryness under nitrogen gas and reconstituted in 500 µL acetonitrile (Duskan, LC-MS grade).

Section S3. UPLC-MS operation, data processing, and statistical analysis

Chromatographic separation was performed on a Kinetex HILIC LC column (100 × 2.1 mm, 2.6 µm, 100 Å, Phenomenex). The flow rate was fixed at 0.3 mL/min with ultra-pure water containing 5 mM ammonium acetate (Fisher, LC-MS grade) as mobile phase A and acetonitrile (Duskan, LC-MS grade) for mobile phase B. The following gradient program was used: 0 to 2 min 95% A; 2 to 4 min linear gradient to 80% B; 4 to 11 min linear gradient to

65% B; 11 to 12.5 min 65% B; 12.5 to 13 min linear gradient to 95% B; 13 to 15 min equilibration wash with 95% B. Injection volume was set at 10 uL. The information dependent analysis (IDA) acquisition was acquired with MS scan (100 to 1200 m/z) followed by MS/MS scan (50 to 1200 m/z) in positive ion mode. The following MS conditions were used: 30 PSI curtain gas, 60 PSI ion source gas, 3000 V ESI ion spray voltage, 320 ℃ source temperature, 10 V collision energy for MS, and 80 V declustering potential. MS/MS was acquired with a collision energy was 20 V with 5 V spread. The raw MS data was processed for peak detection, retention time correction, alignment, and integration using the XCMS software built into the web-based Galaxy platform (https://umsa.cerit-sc.cz/) (Gowda et al., 2014). The processed data was then uploaded to MetaboAnalyst 5.0 (https://www.metaboanalyst.ca/) (Pang et al., 2021) to identify cellular compounds that had prominent ion intensities.

The raw UPLC-MS data first underwent preprocessing, normalization, and quality control steps using the XCMS software built into the web-based Galaxy platform (available at: https://umsa.cerit-sc.cz/). The raw data was processed for peak detection, alignment, and framing. This generated a table that displayed the retention time, mass-to-charge ratio (m/z), and the intensity/peak area for each peak. The quality control step was performed to assess the stability of the intensities of peaks ("features") between samples. This was performed using quality control samples, which were mixtures of equal amounts of experimental samples taken at each time point of the experiment. The relative standard deviation (RSD) of each feature in the quality control sample was compared to those in the experimental samples. Features with higher RSD in the quality control sample than in the experimental samples were excluded, while features with RSD < 30% were retained for further analysis. Multivariable statistical analysis was performed on the retained features using principal component analysis (PCA) with 95% confidence ellipse and partial least squares discrimination analysis (PLS-DA) to identify potential discriminations between the experimental samples. Heatmaps were generated to determine how the retained features changed at different time points during the experiment. A selection of discriminant ions and buckets was done based on the variable importance in projection (VIP) values. Features with VIP values greater than 1.0 were used for the identification step. MS/MS analysis was performed for the structural identification of

compounds. The structure of each compound was deduced based on its adducts, isotopes, and MS/MS fragments using the SCIEX OS-Q software (AB Sciex). Information about compounds' chemical structures, m/z, and retention times were subsequently uploaded to MetaboAnalyst 5.0 (https://www.metaboanalyst.ca/), which used this information to identify the compounds.

Section S4. IC operation

Organic acid concentrations were measured using a Dionex ICS-1100 (ThermoFisher Scientific) system. Separation was achieved using a Dionex IonPac AS18 (4 × 250 mm) anion exchange column (Thermo Scientific) equipped with a Dionex IonPac AG18 (4 × 50 mm) guard column (Thermo Scientific). 16 mM potassium hydroxide (Fisher, ≥85%) was used as the mobile phase at a flow rate of 1.0 mL/min for a 30 min run time. Each aliquot of solution was passed through a syringe filter before IC analysis.

Section S5. Estimation of biodegradation and chemical reaction rates (M s^{-1}) in cloud water

S5.1. Biodegradation

The decay in the concentration of a specific organic acid as a function of time (0 to 12 hours) during a biodegradation experiment can be described by the following equation:

$$\frac{d[Acid]}{dt} = k'_{cell} \times [Acid] = k_{cell,acid} \times [cell]_{experiment} \times [Acid]_{experiment}$$

where k'_{cell} (s^{-1}) is the pseudo first order rate constant obtained from fitting the decay of the organic acid, and $[Acid]_{experiment}$ ($mol\ L^{-1}$) is the initial concentration of the organic acid used in the biodegradation experiment. k'_{cell} is the product of the concentration of bacteria cells used in the experiment ($[cell]_{experiment}, cell\ L^{-1}$) and the biodegradation rate constant ($k_{cell,acid}$, $L\ cell^{-1}s^{-1}$).

The loss rate of the organic acid in cloud water resulting from biodegradation is:

$$\frac{d[Acid]_{cloud}}{dt} = k_{cell,acid} \times [cell]_{cloud} \times [Acid]_{cloud}$$

Deleted: Carboxylic

Deleted: Section S5. Possible enzymes and mechanisms associated with carboxylic acid biodegradation by the two bacterial strains¶

Table S4 summarized enzymes or metabolic pathways related to the biodegradation of carboxylic acids. Genes encoding formate dehydrogenases were identified in both genomes, which is consistent with the observed formate biodegradation. However, no known genes for oxalic acid biodegradation (Liu et al., 2021) were found in the genomes of both strains, which suggested the presence of yet to be characterized pathways that catalyzed the biodegradation. Interestingly, a protein with Cupin 2 domain was found in both genomes. The Cupin superfamily consists of a diverse range of enzymes including oxalate oxidase and oxalate decarboxylase that can biodegrade oxalic acid (Burrell et al., 2007). ¶

Only the *E. hormaechei* B0910 strain was observed to biodegrade malonic acid. Interestingly, the malonyl-CoA-acyl carrier transcacylase observed in the *E. hormaechei* pf0910 strain seems to be a fusion protein, which may render it ineffective in utilizing malonic acid. Although no gene encoding maleate isomerase was identified in the genomes of both strains, the maleic acid biodegradation observed can be attributed to the activity of other enzymes with broad substrates specificity (Hatakeyama et al., 2000). The genes encoding for the small and large protein subunits that together form the 3-isopropylmalate dehydratase, the enzyme that isomerizes 2-isopropylmalate to 3-isopropylmalate, were found in both the *Enterobacter* strains. The small and large protein subunits of this enzyme are homologous to the small (51% amino acid identity) and large (59% amino acid identity) protein subunit constituents of maleate hydratase (HbzIJ) from *Pseudomonas alcaligenes* NCIMB 9867 that converts maleate to D-malate (Liu et al., 2015). Given the high protein homology, we speculate that the 3- ...

Deleted: S6

Deleted: S6

Deleted: carboxylic

Deleted: carboxylic

Deleted: carboxylic

Deleted: carboxylic

where $[cell]_{cloud}$ $(cell\ L^{-1})$ is the concentration of bacteria cells present in cloud water, and $[Acid]_{cloud}$ $(mol\ L^{-1})$ is the concentration of the organic in cloud water.

S5.2. Chemical reactions

The loss rates of the organic acid in cloud water resulting from reactions with ·OH and NO_3· are:

$$\frac{d[Acid]_{cloud}}{dt} = k_{OH,acid} \times [\cdot OH]_{cloud} \times [Acid]_{cloud}$$

$$\frac{d[Acid]_{cloud}}{dt} = k_{NO3,acid} \times [NO_3\cdot]_{cloud} \times [Acid]_{cloud}$$

where $k_{OH,acid}$ $(L\ mol^{-1}s^{-1})$ and $k_{NO3,acid}$ $(L\ mol^{-1}s^{-1})$ are the rate constants for the reactions of the organic acid with ·OH and NO_3·, respectively, and $[\cdot OH]_{cloud}$ $(mol\ L^{-1})$ and $[NO_3\cdot]_{cloud}$ $(mol\ L^{-1})$ are the concentrations of ·OH and NO_3· in cloud water, respectively.

Section S6. Gas-aqueous phase partitioning of monocarboxylic and dicarboxylic acids

Meskhidze et al. (2003) and Guo et al. (2016) previously introduced the concept of "S curves", which describe how the pH of the aqueous phase affects the gas-aqueous partitioning of acidic and basic species. It is assumed that the equilibrium between gas and aqueous phases involves the dissolution of the acidic/basic species into the aqueous phase, followed by the dissociation of the dissolved species. Assuming unity activity coefficients, for monocarboxylic acids (HA, e.g., formic acid), the pH-dependence of the molar fraction of HA in the aqueous phase ($\varepsilon(HA(aq))$) is described by the following equation (Nah et al., 2018):

$$\varepsilon(HA(aq)) = \frac{H_{HA}WRT(10^{-pH} + K_{a1}) \times 0.987 \times 10^{-14}}{10^{-pH} + H_{HA}WRT(10^{-pH} + K_{a1}) \times 0.987 \times 10^{-14}}$$

where W is liquid water concentration (μg m^{-3}), H_{HA} (mole L^{-1} atm^{-1}) is the Henry's law constants for monocarboxylic acid, K_{a1} (mole L^{-1}) is the first acid dissociation constant, R is the gas constant (8.314 m^3 Pa K^{-1} mol^{-1}), and T is temperature (K). The complete derivation for $\varepsilon(HA(aq))$ can be found in the SI of Guo et al. (2015).

Assuming unity activity coefficients, for dicarboxylic acids (H_2A, e.g., oxalic acid,

Deleted: $(cell\ L^{-1})$
Deleted: carboxylic
Deleted: S6
Deleted: carboxylic
Deleted: carboxylic
Formatted: Font: Bold
Formatted: Font: 12 pt
Formatted: Superscript
Formatted: Font: 12 pt
Formatted: Font: 12 pt
Formatted: Font: 12 pt
Formatted: Font: 12 pt
Formatted: Indent: First line: 0"
Formatted: Font: 12 pt
Formatted: Font: 12 pt
Formatted: Font: 12 pt
Formatted: Font: 12 pt
Formatted: Font: 12 pt
Formatted: Font: 12 pt
Formatted: Subscript
Formatted: Font: 12 pt

malonic acid, and maleic acid), the pH-dependence of the molar fraction of H_2A in the aqueous phase ($\varepsilon(H_2A(aq))$) can eventually be simplified to the following equation (Nah et al., 2018):

$$\varepsilon(H_2A(aq)) \cong \frac{H_{H_2A}WRT(10^{-pH} + K_{a1}) \times 0.987 \times 10^{-14}}{10^{-pH} + H_{H_2A}WRT(10^{-pH} + K_{a1}) \times 0.987 \times 10^{-14}}$$

where W is liquid water concentration (μg m^{-3}), H_{H_2A} (mole L^{-1} atm^{-1}) is the Henry's law constants for monocarboxylic acid, K_{a1} (mole L^{-1}) is the first acid dissociation constant, R is the gas constant (8.314 m^3 Pa K^{-1} mol^{-1}), and T is temperature (K). The complete derivation for $\varepsilon(H_2A(aq))$ can be found in the SI of Nah et al. (2018), which also includes discussions of the assumptions made during the derivation process which will lead to the disappearance of the second acid dissociation constant (K_{a2}) term during the process of simplifying the equation.

Formatted: Font: 12 pt
Formatted: Font: 12 pt
Formatted: Font: 12 pt
Formatted: Font: 12 pt
Formatted: Font: 12 pt
Formatted: Font: 12 pt
Formatted: Font: 12 pt
Formatted: Font: 12 pt
Formatted: Font: 12 pt
Formatted: Font: 12 pt
Formatted: Font: 12 pt
Formatted: Font: 12 pt
Formatted: Font: 12 pt
Formatted: Font: 12 pt
Formatted: Font: 12 pt
Formatted: Font: 12 pt
Formatted: Font: 12 pt

References

Amato, P., Ménager, M., Sancelme, M., Laj, P., Mailhot, G., and Delort, A.-M.: Microbial population in cloud water at the Puy de Dôme: Implications for the chemistry of clouds, Atmospheric Environment, 39, 4143-4153, https://doi.org/10.1016/j.atmosenv.2005.04.002, 2005.

Amato, P., Joly, M., Besaury, L., Oudart, A., Taib, N., Mone, A. I., Deguillaume, L., Delort, A. M., and Debroas, D.: Active microorganisms thrive among extremely diverse communities in cloud water, PLoS One, 12, e0182869, 10.1371/journal.pone.0182869, 2017.

Anglada, J. M., Martins-Costa, M., Francisco, J. S., and Ruiz-Lopez, M. F.: Interconnection of reactive oxygen species chemistry across the interfaces of atmospheric, environmental, and biological processes, Accounts of chemical research, 48, 575-583, https://doi.org/10.1021/ar500412p, 2015.

Ariya, P. A., Nepotchatykh, O., Ignatova, O., and Amyot, M.: Microbiological degradation of atmospheric organic compounds, Geophysical Research Letters, 29, 34-31-34-34, 10.1029/2002gl015637, 2002.

Attard, E., Yang, H., Delort, A. M., Amato, P., Pöschl, U., Glaux, C., Koop, T., and Morris, C. E.: Effects of atmospheric conditions on ice nucleation activity of Pseudomonas, Atmospheric Chemistry and Physics, 12, 10667-10677, https://doi.org/10.5194/acp-12-10667-2012, 2012.

Aziz, R. K., Bartels, D., Best, A. A., DeJongh, M., Disz, T., Edwards, R. A., Formsma, K., Gerdes, S., Glass, E. M., and Kubal, M.: The RAST Server: rapid annotations using subsystems

technology, BMC genomics, 9, 1-15, https://doi.org/10.1186/1471-2164-9-75, 2008.

Bauer, H., Kasper-Giebl, A., Loflund, M., Giebl, H., Hitzenberger, R., Zibuschka, F., and Puxbaum, H.: The contribution of bacteria and fungal spores to the organic carbon content of cloud water, precipitation and aerosols, Atmospheric Research, 64, 109-119, https://doi.org/10.1016/s0169-8095(02)00084-4, 2002.

Bearson, S., Bearson, B., and Foster, J. W.: Acid stress responses in enterobacteria, Fems Microbiology Letters, 147, 173-180, https://doi.org/10.1111/j.1574-6968.1997.tb10238.x, 1997.

Bianco, A., Voyard, G., Deguillaume, L., Mailhot, G., and Brigante, M.: Improving the characterization of dissolved organic carbon in cloud water: Amino acids and their impact on the oxidant capacity, Sci Rep, 6, 37420, 10.1038/srep37420, 2016.

Bianco, A., Deguillaume, L., Chaumerliac, N., Vaitilingom, M., Wang, M., Delort, A. M., and Bridoux, M. C.: Effect of endogenous microbiota on the molecular composition of cloud water: a study by Fourier-transform ion cyclotron resonance mass spectrometry (FT-ICR MS), Sci Rep, 9, 7663, 10.1038/s41598-019-44149-8, 2019.

Bianco, A., Deguillaume, L., Vaitilingom, M., Nicol, E., Baray, J. L., Chaumerliac, N., and Bridoux, M.: Molecular Characterization of Cloud Water Samples Collected at the Puy de Dome (France) by Fourier Transform Ion Cyclotron Resonance Mass Spectrometry, Environmental Science & Technology, 52, 10275-10285, https://doi.org/10.1021/acs.est.8b01964, 2018.

Burrows, S. M., Elbert, W., Lawrence, M. G., and Poschl, U.: Bacteria in the global atmosphere - Part 1: Review and synthesis of literature data for different ecosystems, Atmospheric Chemistry and Physics, 9, 9263-9280, https://doi.org/10.5194/acp-9-9263-2009, 2009.

Chen, X., Ran, P., Ho, K., Lu, W., Li, B., Gu, Z., Song, C., and Wang, J.: Concentrations and Size Distributions of Airborne Microorganisms in Guangzhou during Summer, Aerosol and Air Quality Research, 12, 1336-1344, https://doi.org/10.4209/aaqr.2012.03.0066, 2012.

Chen, Y., Nie, F., Xie, S.-Q., Zheng, Y.-F., Dai, Q., Bray, T., Wang, Y.-X., Xing, J.-F., Huang, Z.-J., and Wang, D.-P.: Efficient assembly of nanopore reads via highly accurate and intact error correction, Nature Communications, 12, 1-10, https://doi.org/10.1038/s41467-020-20236-7, 2021.

Clegg, S. L., Brimblecombe, P., and Khan, L.: The Henry's law constant of oxalic acid and its partitioning into the atmospheric aerosol, Idojaras, 100, 51-68, 1996.

Coelho, C. H., Allen, A. G., Fornaro, A., Orlando, E. A., Grigoletto, T. L., and Campos, M. L. A.: Wet deposition of major ions in a rural area impacted by biomass burning emissions, Atmospheric environment, 45, 5260-5265, https://doi.org/10.1016/j.atmosenv.2011.06.063, 2011.

Compernolle, S. and Müller, J. F.: Henry's law constants of diacids and hydroxy polyacids: recommended values, Atmos. Chem. Phys., 14, 2699-2712, https://doi.org/10.5194/acp-14-2699-2014, 2014.

Davey, M. E. and O'toole, G. A.: Microbial biofilms: from ecology to molecular genetics, Microbiology and molecular biology reviews, 64, 847-867, https://doi.org/10.1128/MMBR.64.4.847-867.2000, 2000.

Delort, A.-M., Vaïtilingom, M., Amato, P., Sancelme, M., Parazols, M., Mailhot, G., Laj, P., and Deguillaume, L.: A short overview of the microbial population in clouds: Potential roles in atmospheric chemistry and nucleation processes, Atmospheric Research, 98, 249-260, 10.1016/j.atmosres.2010.07.004, 2010.

Després, V., Huffman, J. A., Burrows, S. M., Hoose, C., Safatov, A., Buryak, G., Fröhlich-Nowoisky, J., Elbert, W., Andreae, M., Pöschl, U., and Jaenicke, R.: Primary biological aerosol particles in the atmosphere: a review, Tellus B: Chemical and Physical Meteorology, 64, https://doi.org/10.3402/tellusb.v64i0.15598, 2012.

Ding, W., Li, L., Han, Y., Liu, J., and Liu, J.: Site-related and seasonal variation of bioaerosol emission in an indoor wastewater treatment station: level, characteristics of particle size, and microbial structure, Aerobiologia, 32, 211-224, https://doi.org/10.1007/s10453-015-9391-5, 2015.

Ervens, B. and Amato, P.: The global impact of bacterial processes on carbon mass, Atmospheric Chemistry and Physics, 20, 1777-1794, https://doi.org/10.5194/acp-20-1777-2020, 2020.

Ervens, B., Gligorovski, S., and Herrmann, H.: Temperature-dependent rate constants for hydroxyl radical reactions with organic compounds in aqueous solutions, Physical Chemistry Chemical Physics, 5, 1811-1824, https://doi.org/10.1039/B300072A, 2003.

Ervens, B., Turpin, B. J., and Weber, R. J.: Secondary organic aerosol formation in cloud droplets and aqueous particles (aqSOA): a review of laboratory, field and model studies, Atmos. Chem. Phys., 11, 11069-11102, 10.5194/acp-11-11069-2011, 2011.

Fankhauser, A. M., Antonio, D. D., Krell, A., Alston, S. J., Banta, S., and McNeill, V. F.: Constraining the Impact of Bacteria on the Aqueous Atmospheric Chemistry of Small Organic Compounds, ACS Earth and Space Chemistry, 3, 1485-1491, 10.1021/acsearthspacechem.9b00054, 2019.

Flemming, H. C. and Wingender, J.: The biofilm matrix, Nature Reviews Microbiology, 8, 623-633, https://doi.org/10.1038/nrmicro2415, 2010.

George, K. M., Ruthenburg, T. C., Smith, J., Yu, L., Zhang, Q., Anastasio, C., and Dillner, A. M.: FT-IR quantification of the carbonyl functional group in aqueous-phase secondary organic aerosol from phenols, Atmospheric Environment, 100, 230-237, https://doi.org/10.1016/j.atmosenv.2014.11.011, 2015.

Gioda, A., Reyes-Rodriguez, G. J., Santos-Figueroa, G., Collett, J. L., Decesari, S., Ramos, M., Netto, H., Neto, F. R. D., and Mayol-Bracero, O. L.: Speciation of water-soluble inorganic, organic, and total nitrogen in a background marine environment: Cloud water, rainwater, and aerosol particles, Journal of Geophysical Research-Atmospheres, 116, https://doi.org/10.1029/2010jd015010, 2011.

Gowda, H., Ivanisevic, J., Johnson, C. H., Kurczy, M. E., Benton, H. P., Rinehart, D., Nguyen, T., Ray, J., Kuehl, J., Arevalo, B., Westenskow, P. D., Wang, J., Arkin, A. P., Deutschbauer, A. M., Patti, G. J., and Siuzdak, G.: Interactive XCMS Online: simplifying advanced metabolomic data processing and subsequent statistical analyses, Anal Chem, 86, 6931-6939, https://doi.org/10.1021/ac500734c, 2014.

Guan, N. and Liu, L.: Microbial response to acid stress: mechanisms and applications, Applied Microbiology and Biotechnology, 104, 51-65, https://doi.org/10.1007/s00253-019-10226-1, 2020.

Guo, H., Liu, J., Froyd, K. D., Roberts, J. M., Veres, P. R., Hayes, P. L., Jimenez, J. L., Nenes, A., and Weber, R. J.: Fine particle pH and gas–particle phase partitioning of inorganic species in Pasadena, California, during the 2010 CalNex campaign, Atmos. Chem. Phys., 17, 5703-5719, https://doi.org/10.5194/acp-17-5703-2017, 2017.

Guo, H., Sullivan, A. P., Campuzano-Jost, P., Schroder, J. C., Lopez-Hilfiker, F. D., Dibb, J. E., Jimenez, J. L., Thornton, J. A., Brown, S. S., Nenes, A., and Weber, R. J.: Fine particle pH and the partitioning of nitric acid during winter in the northeastern United States, Journal of Geophysical Research: Atmospheres, 121, 10,355-310,376, https://doi.org/10.1002/2016JD025311, 2016.

Haynes, W. M.: CRC handbook of chemistry and physics, CRC Press, Boca Raton, Florida2014.

Herrmann, H., Hoffmann, D., Schaefer, T., Brauer, P., and Tilgner, A.: Tropospheric aqueous-phase free-radical chemistry: radical sources, spectra, reaction kinetics and prediction tools, Chemphyschem, 11, 3796-3822, https://doi.org/10.1002/cphc.201000533, 2010.

Hu, W., Niu, H. Y., Murata, K., Wu, Z. J., Hu, M., Kojima, T., and Zhang, D. Z.: Bacteria in atmospheric waters: Detection, characteristics and implications, Atmospheric Environment, 179, 201-221, https://doi.org/10.1016/j.atmosenv.2018.02.026, 2018.

Huang, D. D., Zhang, Q., Cheung, H. H. Y., Yu, L., Zhou, S., Anastasio, C., Smith, J. D., and Chan, C. K.: Formation and Evolution of aqSOA from Aqueous-Phase Reactions of Phenolic Carbonyls: Comparison between Ammonium Sulfate and Ammonium Nitrate Solutions, Environmental Science & Technology, 52, 9215-9224, https://doi.org/10.1021/acs.est.8b03441, 2018.

Huang, S., Hu, W., Chen, J., Wu, Z., Zhang, D., and Fu, P.: Overview of biological ice nucleating particles in the atmosphere, Environment International, 146, 106197, https://doi.org/10.1016/j.envint.2020.106197, 2021.

566 Huang, X.-F., Li, X., He, L.-Y., Feng, N., Hu, M., Niu, Y.-W., and Zeng, L.-W.: 5-Year study
567 of rainwater chemistry in a coastal mega-city in South China, Atmospheric Research, 97, 185-
568 193, https://doi.org/10.1016/j.atmosres.2010.03.027, 2010.

569 Husárová, S., Vaïtilingom, M., Deguillaume, L., Traikia, M., Vinatier, V., Sancelme, M., Amato,
570 P., Matulová, M., and Delort, A.-M.: Biotransformation of methanol and formaldehyde by
571 bacteria isolated from clouds. Comparison with radical chemistry, Atmospheric Environment,
572 45, 6093-6102, 10.1016/j.atmosenv.2011.06.035, 2011.

573 Jaber, S., Joly, M., Brissy, M., Leremboure, M., Khaled, A., Ervens, B., and Delort, A.-M.:
574 Biotic and abiotic transformation of amino acids in cloud water: experimental studies and
575 atmospheric implications, Biogeosciences, 18, 1067-1080, 10.5194/bg-18-1067-2021, 2021.

576 Jaber, S., Lallement, A., Sancelme, M., Leremboure, M., Mailhot, G., Ervens, B., and Delort,
577 A.-M.: Biodegradation of phenol and catechol in cloud water: comparison to chemical
578 oxidation in the atmospheric multiphase system, Atmospheric Chemistry and Physics, 20,
579 4987-4997, 10.5194/acp-20-4987-2020, 2020.

580 Jaenicke, R.: Abundance of cellular material and proteins in the atmosphere, Science, 308, 73-
581 73, https://doi.org/10.1126/science.1106335, 2005.

582 Jain, C., Rodriguez-R, L. M., Phillippy, A. M., Konstantinidis, K. T., and Aluru, S.: High
583 throughput ANI analysis of 90K prokaryotic genomes reveals clear species boundaries, Nature
584 communications, 9, 1-8, https://doi.org/10.1038/s41467-018-07641-9, 2018.

585 Joly, M., Amato, P., Sancelme, M., Vinatier, V., Abrantes, M., Deguillaume, L., and Delort, A.-
586 M.: Survival of microbial isolates from clouds toward simulated atmospheric stress factors,
587 Atmospheric Environment, 117, 92-98, https://doi.org/10.1016/j.atmosenv.2015.07.009, 2015.

588 Kanehisa, M., Sato, Y., and Kawashima, M.: KEGG mapping tools for uncovering hidden
589 features in biological data, Protein Science, 31, 47-53, https://doi.org/10.1002/pro.4172, 2022.

590 Koutny, M., Sancelme, M., Dabin, C., Pichon, N., Delort, A.-M., and Lemaire, J.: Acquired
591 biodegradability of polyethylenes containing pro-oxidant additives, Polymer Degradation and
592 Stability, 91, 1495-1503, 10.1016/j.polymdegradstab.2005.10.007, 2006.

593 Laszakovits, J. R. and MacKay, A. A.: Data-Based Chemical Class Regions for Van Krevelen
594 Diagrams, Journal of the American Society for Mass Spectrometry, 33, 198-202,
595 https://doi.org/10.1021/jasms.1c00230, 2022.

596 Li, T., Wang, Z., Wang, Y., Wu, C., Liang, Y., Xia, M., Yu, C., Yun, H., Wang, W., Wang, Y.,
597 Guo, J., Herrmann, H., and Wang, T.: Chemical characteristics of cloud water and the impacts
598 on aerosol properties at a subtropical mountain site in Hong Kong SAR, Atmospheric
599 Chemistry and Physics, 20, 391-407, https://doi.org/10.5194/acp-20-391-2020, 2020.

600 Lide, D. R. and Frederikse, H. P. R.: CRC handbook of chemistry and physics, Boca Raton,
601 Florida1995.

602 Löflund, M., Kasper-Giebl, A., Schuster, B., Giebl, H., Hitzenberger, R., and Puxbaum, H.:
603 Formic, acetic, oxalic, malonic and succinic acid concentrations and their contribution to
604 organic carbon in cloud water, Atmospheric Environment, 36, 1553-1558,
605 https://doi.org/10.1016/S1352-2310(01)00573-8, 2002.

606 Lund, P., Tramonti, A., and De Biase, D.: Coping with low pH: molecular strategies in
607 neutralophilic bacteria, FEMS Microbiology Reviews, 38, 1091-1125,
608 https://doi.org/10.1111/1574-6976.12076, 2014.

609 Makuc, J., Paiva, S., Schauen, M., Krämer, R., André, B., Casal, M., Leão, C., and Boles, E.:
610 The putative monocarboxylate permeases of the yeast Saccharomyces cerevisiae do not
611 transport monocarboxylic acids across the plasma membrane, Yeast, 18, 1131-1143, 2001.

612 Manni, M., Berkeley, M. R., Seppey, M., and Zdobnov, E. M.: BUSCO: assessing genomic
613 data quality and beyond, Current Protocols, 1, e323, https://doi.org/10.1002/cpz1.323, 2021.

614 Matulova, M., Husarova, S., Capek, P., Sancelme, M., and Delort, A. M.: Biotransformation of
615 various saccharides and production of exopolymeric substances by cloud-borne Bacillus sp.
616 3B6, Environ Sci Technol, 48, 14238-14247, 10.1021/es501350s, 2014.

617 Meier-Kolthoff, J. P. and Göker, M.: TYGS is an automated high-throughput platform for state-
618 of-the-art genome-based taxonomy, Nature communications, 10, 1-10,
619 https://doi.org/10.1038/s41467-019-10210-3, 2019.

620 Meskhidze, N., Chameides, W. L., Nenes, A., and Chen, G.: Iron mobilization in mineral dust:
621 Can anthropogenic SO2 emissions affect ocean productivity?, Geophysical Research Letters,
622 30, https://doi.org/10.1029/2003GL018035, 2003.

623 Misovich, M. V., Hettiyadura, A. P. S., Jiang, W. Q., Zhang, Q., and Laskin, A.: Molecular-
624 Level Study of the Photo-Oxidation of Aqueous-Phase Guaiacyl Acetone in the Presence of C-
625 3*: Formation of Brown Carbon Products, Acs Earth and Space Chemistry, 5, 1983-1996,
626 https://doi.org/10.1021/acsearthspacechem.1c00103, 2021.

627 Möhler, O., DeMott, P., Vali, G., and Levin, Z.: Microbiology and atmospheric processes: the
628 role of biological particles in cloud physics, Biogeosciences, 4, 1059-1071,
629 https://doi.org/10.5194/bg-4-1059-2007, 2007.

630 Morris, C. E., Soubeyrand, S., Bigg, E. K., Creamean, J. M., and Sands, D. C.: Mapping
631 Rainfall Feedback to Reveal the Potential Sensitivity of Precipitation to Biological Aerosols,
632 Bulletin of the American Meteorological Society, 98, 1109-1118,
633 https://doi.org/10.1175/BAMS-D-15-00293.1, 2017.

634 Morris, C. E., Conen, F., Alex Huffman, J., Phillips, V., Pöschl, U., and Sands, D. C.:
635 Bioprecipitation: a feedback cycle linking earth history, ecosystem dynamics and land use
636 through biological ice nucleators in the atmosphere, Glob Chang Biol, 20, 341-351,
637 https://doi.org/10.1111/gcb.12447, 2014.

638 Nah, T., Guo, H., Sullivan, A. P., Chen, Y., Tanner, D. J., Nenes, A., Russell, A., Ng, N. L.,
639 Huey, L. G., and Weber, R. J.: Characterization of aerosol composition, aerosol acidity, and
640 organic acid partitioning at an agriculturally intensive rural southeastern US site, Atmos. Chem.
641 Phys., 18, 11471-11491, https://doi.org/10.5194/acp-18-11471-2018, 2018.

642 Pang, Z., Chong, J., Zhou, G., de Lima Morais, D. A., Chang, L., Barrette, M., Gauthier, C.,
643 Jacques, P. E., Li, S., and Xia, J.: MetaboAnalyst 5.0: narrowing the gap between raw spectra
644 and functional insights, Nucleic Acids Res, 49, W388-W396,
645 https://doi.org/10.1093/nar/gkab382, 2021.

646 Peng, J., Zhou, S., Xiao, K., Zeng, J., Yao, C., Lu, S., Zhang, W., Fu, Y., Yang, Y., and Bi, X.:
647 Diversity of bacteria in cloud water collected at a National Atmospheric Monitoring Station in
648 Southern China, Atmospheric Research, 218, 176-182,
649 https://doi.org/10.1016/j.atmosres.2018.12.004, 2019.

650 Prokof'eva, T. V., Shoba, S. A., Lysak, L. V., Ivanova, A. E., Glushakova, A. M., Shishkov, V.
651 A., Lapygina, E. V., Shilaika, P. D., and Glebova, A. A.: Organic Constituents and Biota in the
652 Urban Atmospheric Solid Aerosol: Potential Effects on Urban Soils, Eurasian Soil Science, 54,
653 1532-1545, https://doi.org/10.1134/S1064229321100094, 2021.

654 Pye, H. O., Nenes, A., Alexander, B., Ault, A. P., Barth, M. C., Clegg, S. L., Collett Jr, J. L.,
655 Fahey, K. M., Hennigan, C. J., and Herrmann, H.: The acidity of atmospheric particles and
656 clouds, Atmospheric chemistry and physics, 20, 4809-4888, https://doi.org/10.5194/acp-20-
657 4809-2020, 2020.

658 Qu, R. and Han, G.: A critical review of the variation in rainwater acidity in 24 Chinese cities
659 during 1982–2018, Elementa: Science of the Anthropocene, 9,
660 https://doi.org/10.1525/elementa.2021.00142, 2021.

661 Rivas-Ubach, A., Liu, Y., Bianchi, T. S., Tolic, N., Jansson, C., and Pasa-Tolic, L.: Moving
662 beyond the van Krevelen diagram: A new stoichiometric approach for compound classification
663 in organisms, Analytical chemistry, 90, 6152-6160, 2018.

664 Romano, S., Fragola, M., Alifano, P., Perrone, M. R., and Talà, A.: Potential Human and Plant
665 Pathogenic Species in Airborne PM10 Samples and Relationships with Chemical Components
666 and Meteorological Parameters, Atmosphere, 12, 654, https://doi.org/10.3390/atmos12050654,
667 2021.

668 Romano, S., Di Salvo, M., Rispoli, G., Alifano, P., Perrone, M. R., and Tala, A.: Airborne
669 bacteria in the Central Mediterranean: Structure and role of meteorology and air mass transport,
670 Sci Total Environ, 697, 134020, https://doi.org/10.1016/j.scitotenv.2019.134020, 2019.

671 Ruiz-Gil, T., Acuña, J. J., Fujiyoshi, S., Tanaka, D., Noda, J., Maruyama, F., and Jorquera, M.
672 A.: Airborne bacterial communities of outdoor environments and their associated influencing
673 factors, Environment International, 145, 106156, https://doi.org/10.1016/j.envint.2020.106156,
674 2020.

675 Sander, R.: Compilation of Henry's law constants (version 4.0) for water as solvent, Atmos.
676 Chem. Phys., 15, 4399-4981, https://doi.org/10.5194/acp-15-4399-2015, 2015.

677 Saxena, P. and Hildemann, L. M.: Water-soluble organics in atmospheric particles: A critical
678 review of the literature and application of thermodynamics to identify candidate compounds,
679 Journal of Atmospheric Chemistry, 24, 57-109, https://doi.org/10.1007/BF00053823, 1996.

680 Seemann, T.: Prokka: rapid prokaryotic genome annotation, Bioinformatics, 30, 2068-2069,
681 https://doi.org/10.1093/bioinformatics/btu153, 2014.

682 Shah, V., Jacob, D. J., Moch, J. M., Wang, X., and Zhai, S.: Global modeling of cloud water
683 acidity, precipitation acidity, and acid inputs to ecosystems, Atmos. Chem. Phys., 20, 12223-
684 12245, https://doi.org/10.5194/acp-20-12223-2020, 2020.

685 Song, F. and Gao, Y.: Chemical characteristics of precipitation at metropolitan Newark in the
686 US East Coast, Atmospheric Environment, 43, 4903-4913,
687 https://doi.org/10.1016/j.atmosenv.2009.07.024, 2009.

688 Sun, X., Wang, Y., Li, H., Yang, X., Sun, L., Wang, X., Wang, T., and Wang, W.: Organic acids
689 in cloud water and rainwater at a mountain site in acid rain areas of South China, Environ Sci
690 Pollut Res Int, 23, 9529-9539, 10.1007/s11356-016-6038-1, 2016.

691 Sündermann, A., Eggers, L. F., and Schwudke, D.: Liquid Extraction: Bligh and Dyer, in:
692 Encyclopedia of Lipidomics, 1-4, https://doi.org/10.1007/978-94-007-7864-1_88-1, 2016.

693 Tilgner, A., Schaefer, T., Alexander, B., Barth, M., Collett Jr, J. L., Fahey, K. M., Nenes, A.,
694 Pye, H. O., Herrmann, H., and McNeill, V. F.: Acidity and the multiphase chemistry of
695 atmospheric aqueous particles and clouds, Atmospheric Chemistry and Physics, 21, 13483-
696 13536, 2021.

697 Tsai, Y. I. and Kuo, S.-C.: Contributions of low molecular weight carboxylic acids to aerosols
698 and wet deposition in a natural subtropical broad-leaved forest environment, Atmospheric
699 Environment, 81, 270-279, https://doi.org/10.1016/j.atmosenv.2013.08.061, 2013.

700 Tyagi, P., Ishimura, Y., and Kawamura, K.: Hydroxy fatty acids in marine aerosols as microbial
701 tracers: 4-year study on β-and ω-hydroxy fatty acids from remote Chichijima Island in the
702 western North Pacific, Atmospheric Environment, 115, 89-100, 2015.

703 Vaitilingom, M., Amato, P., Sancelme, M., Laj, P., Leriche, M., and Delort, A. M.: Contribution
704 of microbial activity to carbon chemistry in clouds, Appl Environ Microbiol, 76, 23-29,
705 10.1128/AEM.01127-09, 2010.

706 Vaitilingom, M., Deguillaume, L., Vinatier, V., Sancelme, M., Amato, P., Chaumerliac, N., and
707 Delort, A. M.: Potential impact of microbial activity on the oxidant capacity and organic carbon
708 budget in clouds, Proc Natl Acad Sci U S A, 110, 559-564, 10.1073/pnas.1205743110, 2013.

709 Vaïtilingom, M., Attard, E., Gaiani, N., Sancelme, M., Deguillaume, L., Flossmann, A. I.,

Amato, P., and Delort, A.-M.: Long-term features of cloud microbiology at the puy de Dôme (France), Atmospheric Environment, 56, 88-100, https://doi.org/10.1016/j.atmosenv.2012.03.072, 2012.

Vaïtilingom, M., Charbouillot, T., Deguillaume, L., Maisonobe, R., Parazols, M., Amato, P., Sancelme, M., and Delort, A. M.: Atmospheric chemistry of carboxylic acids: microbial implication versus photochemistry, Atmospheric Chemistry and Physics, 11, 8721-8733, 10.5194/acp-11-8721-2011, 2011.

Watson, J., Baker, T., and Bell, S.: Molecular biology of the gene, 6th edn. W, 2007.

Weast, R. C. and Astle, M. J.: CRC Handbook of Chemistry and Physics, CRC Press1981.

Wei, M., Xu, C., Chen, J., Zhu, C., Li, J., and Lv, G.: Characteristics of bacterial community in cloud water at Mt Tai: similarity and disparity under polluted and non-polluted cloud episodes, Atmos. Chem. Phys., 17, 5253-5270, https://doi.org/10.5194/acp-17-5253-2017, 2017.

pKa data compiled by R. Williams: https://organicchemistrydata.org/hansreich/resources/pka/pka_data/pka-compilation-williams.pdf, last access: 7 Dec 2022.

Xu, G., Lee, X., and Lv, Y.: Urban and rural observations of carboxylic acids in rainwater in Southwest of China: the impact of urbanization, Journal of atmospheric chemistry, 62, 249-260, https://doi.org/10.1007/s10874-010-9151-4, 2009.

Zhang, M., Khaled, A., Amato, P., Delort, A. M., and Ervens, B.: Sensitivities to biological aerosol particle properties and ageing processes: potential implications for aerosol–cloud interactions and optical properties, Atmos. Chem. Phys., 21, 3699-3724, https://doi.org/10.5194/acp-21-3699-2021, 2021.

Zhang, Y., Lee, X., and Cao, F.: Chemical characteristics and sources of organic acids in precipitation at a semi-urban site in Southwest China, Atmospheric environment, 45, 413-419, https://doi.org/10.1016/j.atmosenv.2010.09.067, 2011.

Zhao, W., Wang, Z., Li, S., Li, L., Wei, L., Xie, Q., Yue, S., Li, T., Liang, Y., and Sun, Y.: Water-soluble low molecular weight organics in cloud water at Mt. Tai Mo Shan, Hong Kong, Science of the Total Environment, 697, 134095, https://doi.org/10.1016/j.scitotenv.2019.134095, 2019.

Zhou, H., Wang, X., Li, Z., Kuang, Y., Mao, D., and Luo, Y.: Occurrence and Distribution of Urban Dust-Associated Bacterial Antibiotic Resistance in Northern China, Environmental Science & Technology Letters, 5, 50-55, https://doi.org/10.1021/acs.estlett.7b00571, 2018.

Zhu, C., Chen, J., Wang, X., Li, J., Wei, M., Xu, C., Xu, X., Ding, A., and Collett, J. L.: Chemical Composition and Bacterial Community in Size-Resolved Cloud Water at the Summit of Mt. Tai, China, Aerosol and Air Quality Research, 18, 1-14, https://doi.org/10.4209/aaqr.2016.11.0493, 2018.